Published online 8 November 2019 *Nucleic Acids Research, 2019, Vol. 47, No. 22* **11649–11666**
doi: 10.1093/nar/gkz1050

Distinct CoREST complexes act in a cell-type-specific manner

Igor Mačinković[1], Ina Theofel[2], Tim Hundertmark[2], Kristina Kovač[1], Stephan Awe[1], Jonathan Lenz[1], Ignasi Forné[3], Boris Lamp[4], Andrea Nist[4], Axel Imhof[3], Thorsten Stiewe[4], Renate Renkawitz-Pohl[2], Christina Rathke[2] and Alexander Brehm[1,*]

[1]Institute of Molecular Biology and Tumor Research, Biomedical Research Center, Philipps-University, Hans-Meerwein-Strasse 2, 35043, Marburg, Germany, [2]Department of Biology, Philipps-University, Karl-von-Frisch-Strasse 8, 35043, Marburg, Germany, [3]Protein Analysis Unit, BioMedical Center, Faculty of Medicine, Ludwig-Maximilians-University Munich, Großhadernerstrasse 9, 82152 Martinsried, Germany and [4]Genomics Core Facility, Institute of Molecular Oncology, Philipps-University, Hans-Meerwein-Strasse 3, 35043 Marburg, Germany

Received October 31, 2018; Revised October 16, 2019; Editorial Decision October 18, 2019; Accepted October 23, 2019

ABSTRACT

CoREST has been identified as a subunit of several protein complexes that generate transcriptionally repressive chromatin structures during development. However, a comprehensive analysis of the CoREST interactome has not been carried out. We use proteomic approaches to define the interactomes of two dCoREST isoforms, dCoREST-L and dCoREST-M, in *Drosophila*. We identify three distinct histone deacetylase complexes built around a common dCoREST/dRPD3 core: A dLSD1/dCoREST complex, the LINT complex and a dG9a/dCoREST complex. The latter two complexes can incorporate both dCoREST isoforms. By contrast, the dLSD1/dCoREST complex exclusively assembles with the dCoREST-L isoform. Genome-wide studies show that the three dCoREST complexes associate with chromatin predominantly at promoters. Transcriptome analyses in S2 cells and testes reveal that different cell lineages utilize distinct dCoREST complexes to maintain cell-type-specific gene expression programmes: In macrophage-like S2 cells, LINT represses germ line-related genes whereas other dCoREST complexes are largely dispensable. By contrast, in testes, the dLSD1/dCoREST complex prevents transcription of germ line-inappropriate genes and is essential for spermatogenesis and fertility, whereas depletion of other dCoREST complexes has no effect. Our study uncovers three distinct dCoREST complexes that function in a lineage-restricted fashion to repress specific sets of genes thereby maintaining cell-type-specific gene expression programmes.

INTRODUCTION

Multisubunit protein complexes that regulate chromatin activity often form families of related complexes that share a set of core subunits (1). This common core can associate with different accessory subunits to yield alternative complexes with new functionality.

The *RE1 silencing transcription factor* (REST) cooperates with the *corepressor of REST* (CoREST) to silence neuron-specific genes in non-neuronal cell types (2). CoREST is an integral component of multi-subunit *lysine-specific demethylase 1 (LSD1)* complexes which modify nucleosomes by histone deacetylation and demethylation to repress transcription (3–7). The precise composition of LSD1/CoREST complexes differs depending on cell type and purification conditions. However, several core subunits have been identified in independent studies (5,6). These include CoREST, LSD1, histone deacetylases HDAC1 and HDAC2, CtBP1, ZNF217, BHC80 and BRAF35.

CoREST and LSD1 are also part of distinct molecular assemblies. Together with SFMBT1 they form the *SFMBT1-LSD1-CoREST* (SLC) complex which represses histone genes in a cell-cycle-dependent manner (8). In addi-

*To whom correspondence should be addressed. Tel: +49 6421 2866840; Fax: +49 6421 2866842; Email: brehm@imt.uni-marburg.de
Present addresses:
Ina Theofel, MRC London Institute of Medical Sciences (LMS), Institute of Clinical Sciences (ICS), Faculty of Medicine, Imperial College London, Du Cane Road, London W120NN, UK.
Kristina Kovač, Department of Biology, Stanford University, 371 Serra Mall, Stanford, CA 94305, USA.
Christina Rathke, Dekanat Fachbereich Medizin, Justus-Liebig-University, Klinikstr. 29, Gießen, Germany.

tion, LSD1 and CoREST coexist with SIRT1 in a complex that represses Notch target genes (9).

The co-existence of LSD1 and CoREST in all of the complexes described above suggests that these two proteins form a core that can associate with different accessory subunits. So far, LSD1 and CoREST have not been demonstrated to exist in separate complexes in mammals.

Both CoREST and LSD1 are conserved in *Drosophila*. Genetic studies imply that they cooperate in the differentiation of wing structures and ovarian follicle cells by regulating signalling pathways including Notch and DPP/TGFbeta (9–12). These observations suggest that *Drosophila* LSD1/CoREST complexes exist that are similar to their mammalian counterparts. In support of this notion, dLSD1 and dCoREST interact when overexpressed in S2 cells and both proteins are associated in ovary extracts (12,13). However, dLSD1/dCoREST complexes are poorly characterized. Indeed, several subunits of mammalian LSD1/CoREST complexes do not have apparent homologues in *Drosophila* (e.g. ZNF217, BHC80 and BRAF35) raising questions about the existence and subunit composition of putative dLSD1/dCoREST complexes.

The only *Drosophila* CoREST-containing complex biochemically characterized to date is the L(3)mbt-interacting (LINT) complex which functions to prevent the expression of lineage-inappropriate genes in both ovaries and in Kc cells (14,15). LINT consists of dL(3)mbt, the dL(3)mbt-interacting protein 1 (dLint-1), the histone deacetylase dRPD3 and dCoREST (15). Notably, dLSD1 is not a stoichiometric subunit of LINT and is not required to repress LINT target genes (15). The existence of additional dCoREST complexes has not been systematically analysed.

The *dCoREST* gene expresses two major isoforms by alternative splicing, dCoREST-L and dCoREST-M (Figure 1A; (13)). Both isoforms contain an ELM2 domain and two SANT domains. dCoREST-L is characterized by a 234 amino acid insertion in the linker that is separating the two SANT domains that is absent in dCoREST-M. It is unknown, if these two isoforms reside in different complexes or are fully redundant.

In this study, we systematically define the interactome of dCoREST in *Drosophila* cells. We use gel filtration, immunoaffinity purification, mass spectrometry and reconstitution from recombinant subunits to identify three distinct dCoREST-containing complexes: the LINT complex described above, a stable dLSD1/dCoREST complex and a dG9a/dCoREST complex. Whereas LINT subunits and dG9a interact with both dCoREST-L and dCoREST-M, dLSD1 displays a striking isoform specificity and associates exclusively with dCoREST-L. We employ ChIP-seq and RNA interference combined with RNA-seq to systematically identify the genome-wide distribution of dCoREST complexes and their target genes. Strikingly, our results identify LINT as the major effector of dCoREST-mediated transcriptional repression in macrophage-like S2 cells, whereas spermatogenesis and maintenance of a germ line-specific gene expression programme rely exclusively on the dLSD1/dCoREST complex. Collectively, our data support the model that different cell lineages employ specific dCoREST complexes to generate and maintain their cell-type-specific transcriptional programmes.

MATERIALS AND METHODS

Cell culture

Spodoptera frugiperda Sf9, *Drosophila melanogaster* S2 and *D. melanogaster* S2[Cas9] (kind gift from Klaus Förstemann, Munich) cell lines were maintained in Sf-900 medium (Gibco) and Schneider's medium (Gibco), respectively, supplemented with 10% (v/v) Fetal calf serum (Sigma) and 1% (v/v) Penicillin-Streptomycin (Gibco) under standard conditions (26°C).

Nuclear extract preparation

S2 cells were harvested, washed in phosphate-buffered saline (PBS) and resuspended in three volumes of low salt buffer (10 mM Hepes pH 7.6, 1.5 mM $MgCl_2$, 10 mM KCl, 1.0 mM dithiothreitol (DTT)). After incubation on ice for 10 min, cells were collected by centrifugation at 21 100 × *g* for 1 min at 4°C. The supernatant was discarded, and nuclei were resuspended in 1.5 volumes of high salt buffer (20 mM Hepes pH 7.6, 1.5 mM $MgCl_2$, 420 mM NaCl, 0.2 mM ethylenediaminetetraacetic acid (EDTA), 20% (v/v) glycerol, 1.0 mM DTT). The suspension was incubated for 20 min on ice and subsequently centrifuged at 21 100 × *g* for 30 min at 4°C. The supernatant (nuclear extract) was aliquoted, frozen in liquid nitrogen and stored at −80°C.

Preparation of nuclear extract from *Drosophila* embryos was done as described previously (16).

The protein concentration of nuclear extracts was determined using Protein Assay Dye Reagent (Bio-Rad) according to the manufacturer's instructions using BSA (Roth) as a standard.

Gel filtration

A total of 1 mg of S2 nuclear extract or embryo (0–12 h after egg deposition) nuclear extract were applied to a Superose 6 HR 10/30 gel filtration column (GE Healthcare) using a 200-μl sample loading loop on an Äkta purifier system (GE Healthcare). Samples were resolved in 10 mM Hepes pH 7.6, 1.5 mM MgCl2, 300 mM KCl, 0.5 mM EGTA and 10% (v/v) glycerol and 0.5 ml fractions were collected with a F9-R fraction collector following the manufacturer's instructions. Fractions were precipitated using 5 μl StrataClean resin (Agilent) or immunoprecipitated using GFP-Trap® (Chromotek) and subjected to western blot analysis. Elution volumes of proteins with known molecular weights were determined using the Gel Filtration Calibration Kit (GE Healthcare) according to the manufacturer's instructions.

Co-immunoprecipitations

Anti-GFP (Chromotek) co-immunoprecipitation of fractions (0.5 ml) collected after gel filtration was performed according to the manufacturer's instructions. The fractions were diluted 1:1 with 10 mM Hepes pH 7.6, to lower the salt concentration of KCl to 150 mM and incubated with 25 μl of equilibrated GFP-Trap® overnight at 4°C. Unbound proteins were removed by washing four times with IP-150 buffer (25 mM Hepes pH 7.6, 12.5 mM $MgCl_2$, 150

mM NaCl, 0.1 mM EDTA, 10% (v/v) glycerol, 0.1% (v/v) NP-40) for 5 min, and the bound proteins were eluted by incubating the beads with 30 μl of 1× NuPAGE® LDS Sample Buffer (Invitrogen). A total of 20 μl of the eluate was analysed by western blot.

For co-immunoprecipitation of endogenous dCoREST, anti-CoREST rabbit polyclonal antibody was cross-linked to Protein G Sepharose (GE Healthcare) and co-immunoprecipitation was performed as previously described (17). In brief, four independent cross-linking reactions were prepared using 30 μg of anti-CoREST rabbit polyclonal antibody or 30 μg of IgG (Normal Rabbit IgG, Cell Signalling) and 70 μl of Protein G Sepharose (GE Healthcare). Additionally, the beads were blocked for 1 h with 1% Gelatin from cold water fish skin (Sigma) and 0.2 mg/ml Albumin from chicken egg white (Sigma). Cross-linked beads were incubated overnight with 6 mg of S2 nuclear extract. Unbound proteins were removed by washing three times with high salt buffer supplemented with 0.05% NP-40 (Fluka) for 5 min, followed by washing with high salt buffer and finally two washes with 50 mM $(NH_4)HCO_3$ (Roth). About 10% of the affinity-purified material was electrophoresed and analysed by silver staining (SilverQuest™ Staining Kit, Invitrogen) and the rest was subjected to LC-MS/MS analysis.

Anti-FLAG (Sigma) co-immunoprecipitation was performed according to the manufacturer's instructions in high salt buffer. A total of 200 μl of anti-FLAG® M2 Affinity Gel was equilibrated and blocked for 1 h with 1% Gelatin from cold water fish skin (Sigma) and 0.2 mg/ml Albumin from chicken egg white (Sigma) in high salt buffer. A total of 10 mg of S2 nuclear extract was incubated overnight with 200 μl of beads. Unbound proteins were removed by washing three times with high salt buffer supplemented with 0.05% NP-40 (Fluka) for 5 min, followed by washing with high salt buffer and finally two washes with 50 mM $(NH_4)HCO_3$ (Roth). 10% of the affinity-purified material was electrophoresed and analysed by silver staining (SilverQuest™ Staining Kit, Invitrogen), 10% of the affinity-purified material was electrophoresed and analysed by western blot. The rest (80%) was subjected to LC-MS/MS analysis.

LC-MS/MS analysis

LC-MS/MS sample preparation and analysis was carried out according to methods described in (18). Briefly, after immunoaffinity purification, beads were washed with 50 mM $(NH_4)HCO_3$ and incubated with 10 ng/μl Trypsin in 1 M urea, 50 mM $(NH_4)HCO_3$ for 30 min, washed with 50 mM $(NH_4)HCO_3$ and the supernatant was digested overnight in the presence of 1 mM DTT. Digested peptides were alkylated and desalted prior to LC-MS/MS analysis.

For LC-MS/MS purposes, desalted peptides were injected in an Ultimate 3000 RSLCnano system (Thermo), separated in a 15-cm analytical column (75 μm ID home-packed with ReproSil-Pur C18-AQ 2.4 μm from Dr Maisch) with a 50-min gradient from 5 to 60% acetonitrile in 0.1% formic acid. The effluent from the HPLC was directly electrosprayed into a Qexactive HF (Thermo) operated in data dependent mode to automatically switch between full scan MS and MS/MS acquisition. Survey full scan MS spectra (from m/z 375–1600) were acquired with resolution $R = 60\,000$ at m/z 400 (AGC target of 3×10^6). The 10 most intense peptide ions with charge states between 2 and 5 were sequentially isolated to a target value of 1×10^5, and fragmented at 27% normalized collision energy. Typical mass spectrometric conditions were: spray voltage, 1.5 kV; no sheath and auxiliary gas flow; heated capillary temperature, 250°C; ion selection threshold, 33.000 counts. MaxQuant 1.5.2.8 was used to identify proteins and quantify by iBAQ with the following parameters: Database, Uniprot_0803_Dmelanogaster_20180723; MS tol, 10ppm; MS/MS tol, 20ppm; Peptide FDR, 0.1; Protein FDR, 0.01 Min. peptide Length, 5; Variable modifications, Oxidation (M); Fixed modifications, Carbamidomethyl (C); Peptides for protein quantitation, razor and unique; Min. peptides, 1; Min. ratio count, 2. Identified proteins were analysed in Perseus with a *t*-test adjusted for multiple comparisons.

Antibodies

dCoREST (G. Mandel), dLSD1 (dSu(var)3–3; G. Reuter) and dG9a (M. Yamaguchi) antibodies were generous gifts. Rabbit polyclonal anti-dL(3)mbt, anti-dLint-1, anti-dMi-2 (anti-dMi2-Nterm), anti-dRpd3 and anti-MstF77 antibodies have been previously described (15,19). Anti-beta-Tubulin (clone KMX-1), anti-FLAG rabbit polyclonal antibody and anti-FLAG M2 agarose were purchased from Millipore and Sigma Aldrich, respectively. Anti-GFP was purchased from Chromotek.

HRP linked anti-Mouse IgG (Amersham, NA931), anti-rabbit IgG (Amersham, NA934) or anti-rat IgG (Invitrogen, 31470) secondary antibodies were used to visualize western blot signals by chemiluminescence using the Immobilon Western Chemiluminescence HRP substrate (Millipore, WBKLS0500).

Chromatin Immunoprecipitation

Exponentially growing S2[Cas9] cells (1×10^8) expressing GFP-tagged proteins were cross-linked with 1% Formaldehyde (Roth) for 10 min at room temperature. Cross-linking was stopped by adding Glycine to a final concentration of 240 mM and incubating samples for 10 min at room temperature. Cells were then washed twice in PBS and lysed in 1 ml of ChIP Lysis buffer (50 mM Tris/HCl pH 8.0, 10 mM EDTA, 1% (w/v) SDS, 1 mM DTT) for 10 min on ice. Chromatin was sheared by sonication in a Bioruptor UCD-200TM-EX (Diagenode) supplied with ice water. Three sonication cycles were applied, each cycle lasting for 10 min with 30 s intervals of sonication at high power interrupted by 30 s of resting. Cell debris were pelleted by centrifugation (20 min, 21 100 × *g*, 4°C) and the supernatant containing fragmented chromatin was stored at −80°C. The fragment size was monitored by decrosslinking 50 μl of chromatin-containing lysate in the presence of RNase A (400 ng/μl, Applichem) and Proteinase K (400 ng/μl, Applichem) for 3 h at 55°C followed by 65°C over night. DNA was purified using the QIAquick PCR purification kit (Qiagen) and the fragment size was evaluated on a 1.2% Agarose/TAE gel.

For ChIP 1 ml of chromatin lysate was precleared by 1:10 dilution in ChIP IP buffer (16.7 mM Tris/HCl pH 8.0, 1.2

mM EDTA, 167 mM NaCl, 1 mM DTT) and addition of 285 μl Protein A Sepharose resin (GE Healthcare) that had been blocked for 1 h in ChIP Blocking buffer (ChIP Low salt buffer containing 2 mg/ml BSA and 2% (w/v) Gelatin from cold water fish skin). After incubation at 4°C for 1 h with rotation, beads were precipitated (centrifugation for 10 min, 21 100 × *g*, 4°C) and the supernatant was added to 200 μl of blocked GFP-Trap.

Immunoprecipitation took place over night at 4°C with rotation followed by washing: 3× with 15 ml of ChIP Low salt buffer (20 mM Tris/HCl pH 8.0, 2 mM EDTA, 150 mM NaCl, 1% (w/v) Triton X-100, 0.1% (w/v) SDS, 1 mM DTT), 3× with 15 ml of ChIP High salt buffer (20 mM Tris/HCl pH 8.0, 2 mM EDTA, 500 mM NaCl, 1% (w/v) Triton X-100, 0.1% (w/v) SDS, 1 mM DTT), 1× with 15 ml of ChIP LiCl buffer (10 mM Tris/HCl pH 8.0, 1 mM EDTA, 250 mM LiCl, 0.1% (w/v) NP-40, 1 mM DTT), 2× with TE buffer (10 mM Tris/HCl pH 8.0, 1 mM EDTA, 1 mM DTT). Each washing step was performed at 4°C for 5 min with rotation and the resin was precipitated in between by centrifugation (4 min, 400 × *g*, 4°C).

Crosslinked protein–DNA complexes were eluted twice from the resin in 500 μl ChIP Elution buffer (100 mM $NaHCO_3$, 2% (w/v) SDS) for 20 min at RT with rotation followed by 10 min incubation at 95°C. Pooled eluates were 1:1 diluted with 100 mM $NaHCO_3$. As 'input' sample, 14 μl of precleared chromatin was added to 250 μl of ChIP Elution buffer and diluted 1:1 with 100 mM $NaHCO_3$. 5 M NaCL was added to the samples to the final concentration of 40 μM. Protein–DNA complexes were decrosslinked over night at 65°C with agitation. 40 mM Tris/HCl pH 6.8, 1 mM EDTA and 40 ng/μl Proteinase K (Applichem) was added to each sample and proteins were digested at 45°C for 1 h with agitation. The DNA was purified using QIAquick PCR purification kit (Qiagen) and the concentration was determined using Quant-iT™ dsDNA High-Sensitivity Assay Kit according to the manufacturer's instruction.

ChIP-seq

Libraries for ChIP-seq analysis were prepared from 500 pg of DNA using MicroPlex Library Preparation Kit v2 (diagenode) following manufacturer's instructions including library size selection using AMPure XP beads (Beckman Coulter). The quality of sequencing libraries was controlled on a Bioanalyzer 2100 using the Agilent High Sensitivity DNA Kit (Agilent). Pooled sequencing libraries were quantified with digital polymerase chain reaction (PCR) (QuantStudio 3D, Thermo Fisher) and sequenced on the NextSeq 550 platform (Illumina) using a high output v2.5 flow cell and 50 base single reads.

Raw Illumina sequence reads were aligned to *D. melanogaster* genome (BDGP6_dm6, ucsc) with the Bowtie2 tool and peak calling was performed with the MACS2 callpeak tool using the Galaxy Server of University of Giessen (default settings). Peaks were filtered using fold change values ≥ 4 and pileup values ≥ 35. Genomic distribution of the peaks was analysed using CEAS: Enrichment on chromosome tool and diagrams were generated using the Venn Diagram tool of Cistrome Galaxy server.

RNAi treatment in cell culture

RNA interference experiments were performed as in (1,20). Briefly, double-stranded RNA was generated by T7 Polymerase *in vitro* transcription from PCR amplimers generated with T7 promoter-containing primers (Supplementary Table S4) using MEGAscript™ T7 Transcription Kit (ThermoFischer) according to the manufacturer's instruction. Double-stranded RNAs (15 μg) were transfected into S2 cells (1.2×10^6 cells) using Effectene (Qiagen), and the cells were harvested 3 to 4 days after transfection. The efficiency of knock-down was confirmed by qPCR and western blot analysis.

Fly lines and crosses

RNA interference experiments in flies were performed using stocks from the VDCR RNAi Library (http://stockcenter.vdrc.at/control/main) carrying RNAi transgenes under UAS control (VDRC RNAi #: dCoREST – 34179; – 34180 and –104900; dLSD1 – 106147; dL(3)mbt – 104563; dLint-1 – 105932; dG9a – 25473; dCHD3 – 102689; CG9973 – 102273; CG2083 - 110549). For knockdown experiments the GAL4-driver strains *engrailed*-GAL4 (wing) and *bam*-GAL4 (germ line) were used, respectively. All flies were collected as virgins before setting up the crosses. Flies were kept at 26°C in a fly incubator.

RNA-seq analysis

Total RNA from *Drosophila* S2 cells was isolated using the peqGOLD Total RNA Kit (S-Line, peqlab) according to manufacturer's instructions. Total RNA from dissected *Drosophila* testes was isolated using the TRIzol (Invitrogen) reagent according to the manufacturer's protocol. Following chloroform extraction, ethanol precipitation and DNase digestion, RNAs were purified using a RNeasy Mini Kit (Qiagen).

RNA integrity was assessed on an Experion StdSens RNA Chip (Bio-Rad). RNA-seq libraries were prepared using a TruSeq Stranded mRNA Library Prep kit (Illumina). Libraries were quantified on a Bioanalyzer (Agilent Technologies) and were sequenced on an Illumina HiSeq 1500 platform, rapid-run mode, single-read 50 bp (HiSeq SR Rapid Cluster Kit v2, HiSeq Rapid SBS Kit v2, 50 cycles) according to the manufacturer's instructions.

For transcriptome analysis, sequenced reads were aligned to the *D. melanogaster* genome (Ensembl revision 89) using STAR (version 2.4.1a) (21). Fragments per kilobase per million (FPKM) were calculated based on the total raw read count per gene and length of merged exons. For the study with cultured S2 cells, differential expression was assessed using DESeq2 (version 1.12.3) (22). To investigate differential gene expression of pooled *Drosophila* testes, logFC values were calculated between the log2 medians of each group after a constant of 1/60 to avoid undefined algorithms. For both analyses, genes that did not yield a minimum raw count of 50 and a minimum FPKM of 0.3 in at least two samples were discarded due to insufficient coverage. Of the remaining genes, genes were considered differentially expressed if the absolute of the log2 FC was at least 1

(twofold induction/repression) and in case of DESeq2 analysis if the corrected *P*-value was less or equal 0.05.

Phase contrast microscopy and immunofluorescence staining

Triple-bam-GAL4 female virgins (bam-GAL4/bam-GAL4;CyO/Sp;Sb/Bam-GAL4) were crossed with males of appropriate RNAi-lines (CoREST: VDRC-34179/GD and Su(var)3–3: VDRC-10647/KK). Offspring were raised in standard conditions (26°C).

For dissection and imaging up to 1-day old males were used. Only males that were non-Sb (i.e. carried 2xbam-GAL4) were selected. Used undriven RNAi lines as controls (up to 1-day old).

Dissected testes in PBS and mounted whole unfixated testes on lysin-coated slides in PBS were imaged at 10× and 20× magnification in phase contrast using a Leica DMR microscope equipped with Quantifire-X1 camera (Intas Science Imaging Instruments). For imaging spermatocytes testes were squashed by removing PBS from under the coverslip.

Images were processed and assembled in GIMP and Inkscape.

Immunofluorescence staining of squashed testis was carried out essentially as described before (19,23,24).

RESULTS

Different dCoREST-containing protein complexes

Alternative splicing produces two main isoforms of dCoREST in macrophage-like S2 cells: dCoREST-L and dCoREST-M (13). dCoREST-L contains a unique 234 amino acid insertion in the linker region separating the two SANT domains that is absent in dCoREST-M (Figure 1A). We have previously shown that both dCoREST isoforms associate with the malignant brain tumour (MBT) domain-containing protein dL(3)mbt, dLint-1 and the histone deacetylase dRPD3 to form the dL(3)mbt-interacting (LINT) complex (15). We hypothesized that additional dCoREST-containing complexes exist. We used gel filtration of nuclear extracts from S2 cells to test this hypothesis. Indeed, only a minor fraction of dCoREST coeluted with the LINT signature subunit dL(3)mbt (Figure 1B). The bulk of dCoREST-L and dCoREST-M eluted in fractions with high apparent molecular mass (>440 kDa) that contained little or no detectable dL(3)mbt. This suggests that dCoREST is a component of additional protein complexes other than LINT. In addition, we observed that dCoREST-L (main peak in fraction 25) and dCoREST-M (main peak in fraction 19) do not peak in the same fractions indicating that isoform-specific complexes might exist.

We used an antibody recognising both dCoREST isoforms to affinity purify dCoREST-interacting proteins from S2 nuclear extract (13). SDS-PAGE followed by silver staining revealed several proteins that specifically co-purified with dCoREST-L/M but were not detected in controls (Figure 1C; compare lane 3 with lanes 1 and 2). Mass spectrometry analysis (LC-MS/MS) identified 373 proteins as putative dCoREST interactors (Supplementary Table S1). All four components of the LINT complex (dL(3)mbt, dLint-1, dRPD3 and dCoREST) were strongly enriched in the immunoprecipitate (Figure 1D).

An isoform-specific dLSD1/dCoREST complex

In mammalian cells, CoREST is an integral part of the LSD1/CoREST complex (3–7).

In S2 cells, dCoREST-L and dLSD1 can interact when both proteins are overexpressed suggesting that this interaction is conserved between vertebrate and invertebrate species (13). Indeed, our purification of endogenous dCoREST enriched three potential subunits of a putative *Drosophila* LSD1/CoREST complex: dLSD1, dCoREST and the HDAC1/2 homologue dRPD3 (Figure 1D, Supplementary Table S1).

We generated an S2 cell line allowing the inducible expression of FLAG-tagged dLSD1 (Figure 2A). FLAG-affinity purification from nuclear extracts of induced cells revealed that dLSD1 co-purified dRPD3 and dCoREST-L. Whilst this result does not allow us to judge to what extent these interactions are stoichiometric it strongly supports the existence of a dLSD1/dCoREST complex. Strikingly, dCoREST-M was not detected in the dLSD1 immunoprecipitate suggesting that dLSD1 binds dCoREST in an isoform-specific manner.

We next established two S2 cell lines for inducible expression of FLAG-tagged dCoREST-L and FLAG-tagged dCoREST-M, respectively (Supplementary Figure S1). dLSD1 was not detected in the FLAG-dCoREST-M immunoprecipitate by western blot (Figure 2B). By contrast, dLSD1 efficiently co-purified with FLAG-tagged dCoREST-L. This isoform-specificity of the dLSD1 interaction was not observed for subunits of the LINT complex: dL(3)mbt, dLint-1 and dRPD3 all co-precipitated with both dCoREST isoforms. We also subjected FLAG-dCoREST-L and FLAG-dCoREST-M immunoprecipitates to LC-MS/MS analysis. In agreement with the western blot result, the LINT subunits dL(3)mbt and dRPD3, and to a lesser extent also dLint-1, were enriched in the FLAG-dCoREST-L immunoprecipitate (Figure 2C and Supplementary Table S2). Likewise, all three LINT subunits were also enriched in the dCoREST-M immunoprecipitate (Figure 2D and Supplementary Table S3). By contrast, dLSD1 was significantly enriched in the dCoREST-L interactome only.

Finally, we generated baculoviruses expressing recombinant dLSD1, dCoREST-L and dCoREST-M. Pairwise co-infection of Sf9 cells followed by co-immunoprecipitation confirmed that dLSD1 preferentially interacts with dCoREST-L (Supplementary Figure S2). Thus, the isoform-specific interaction of dLSD1 with dCoREST-L can be recapitulated with recombinant proteins.

In summary, our results support the hypothesis that dLSD1 and dCoREST-L, but not dLSD1 and dCoREST-M, form a stable complex.

A novel dG9a/dCoREST complex

In addition to LINT subunits and dLSD1, we identified the H3K9-specific methyltransferase dG9a as one of the most abundant interaction partners of endogenous dCoREST (Figure 1D and Supplementary Table S1). dG9a was

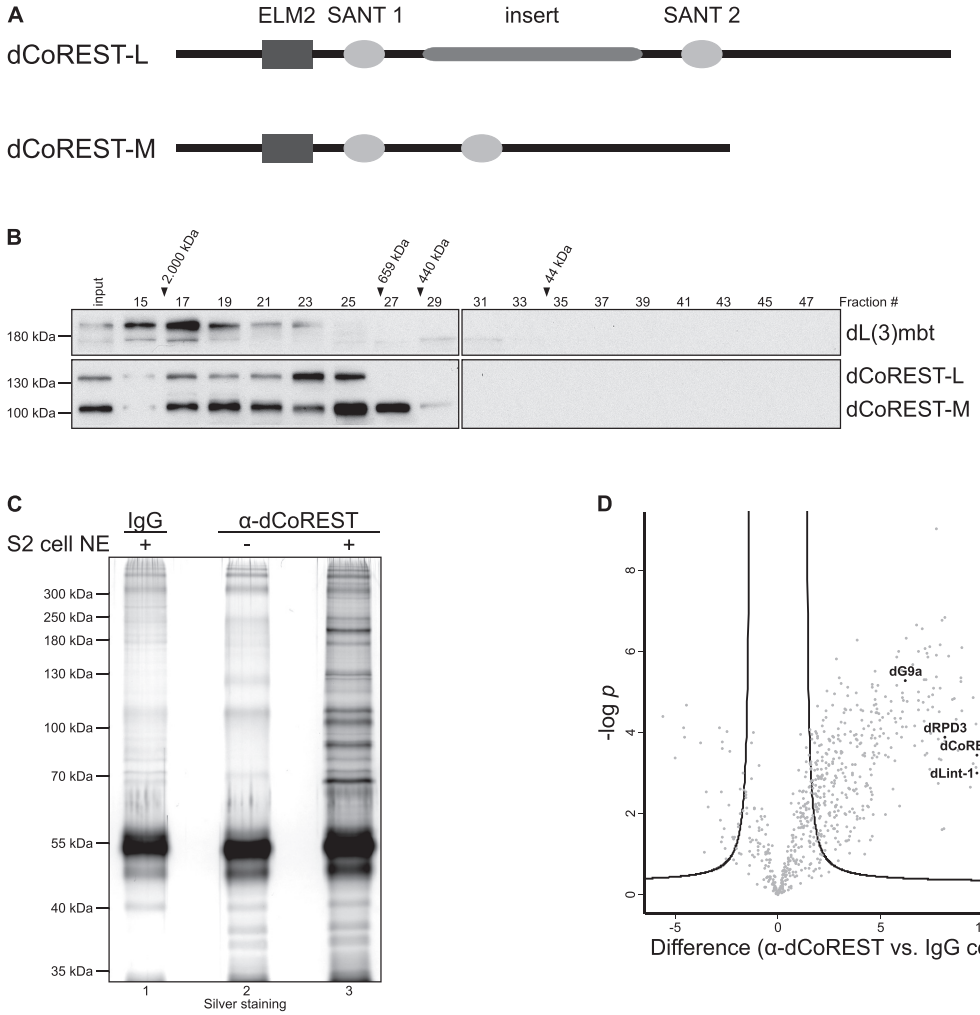

Figure 1. Purification of dCoREST interactors. (**A**) Schematic representation of the two major CoREST protein isoforms in *Drosophila*, dCoREST-L and dCoREST-M. Black rectangles depict ELM2 domains and grey ovals indicate SANT domains. The thick grey line represents a 234 amino acid insert unique to dCoREST-L. (**B**) Nuclear extract from S2 cells was fractionated over a Superose 6 column. Fractions were analysed by western blot using the antibodies indicated on the right. Fraction numbers and molecular mass standards are denoted on top. Input: 5% of extract loaded onto the column. (**C**) Nuclear extracts from S2 cells were subjected to IgG (lane 1) or anti-CoREST (lane 3) affinity purification and the bound material was analysed by sodium dodecyl sulphate-polyacrylamide gelelectrophoresis (SDS-PAGE) and silver staining. As an additional control anti-dCoREST antibody not incubated with nuclear extract was loaded (lane 2). (**D**) Volcano plot with -log10 *P*-values (*y*-axis) and log2 iBAQ fold-difference (*x*-axis) after comparison of anti-CoREST affinity purification versus IgG control. The point labeled 'dCoREST-M' was derived from peptides common to dCoREST-M and dCoREST-L. The point labeled 'dCoREST-L' was derived from peptides mapping the insert region that is exclusive to dCoREST-L. The complete list of the interacting proteins is presented in Supplementary Table S1 ($n = 4$, FDR = 0.01, s0 = 2).

also detected by western blot following the immunoprecipitation of both FLAG-tagged dCoREST isoforms (Figure 2B).

To confirm this interaction we used CRISPR/Cas to add a sequence encoding a GFP-tag to the 3′ end of the endogenous dG9a coding sequence (Supplementary Figure S3 and Table S5). Purification of the resulting dG9a-GFP fusion verified both dCoREST isoforms as well as dRPD3 as interactors of dG9a (Figure 3A). By contrast, neither dL(3)mbt nor dLSD1 were recovered to a significant extent. These results suggest that dG9a is not part of the LINT or dLSD1/dCoREST complexes but forms a separate assembly with dCoREST and dRPD3.

We next asked if dG9a forms a stoichiometric complex with dCoREST. We analysed dG9a-GFP purified from nuclear extracts by SDS-PAGE and silver staining (Figure 3B). This resulted in the co-purification of four polypeptides ranging in apparent molecular masses from 250 to 300 kDa. These masses correspond well to the mass expected for dG9a-GFP. We do not currently know if these polypeptides represent isoforms of dG9a, posttranslationally modified dG9a, degradation products or, indeed, interaction partners. It is clear, however, that this purification did not reveal polypeptides with apparent molecular masses similar to those of dCoREST-L, dCoREST-M or dRPD3 arguing that the bulk of dG9a is not associated with dCoREST and dRPD3. We considered the possibility that addition of the GFP moiety to the C-terminus of endogenous dG9a might disrupt interactions with dCoREST and dRPD3. Therefore, we used CRISPR/Cas to cre-

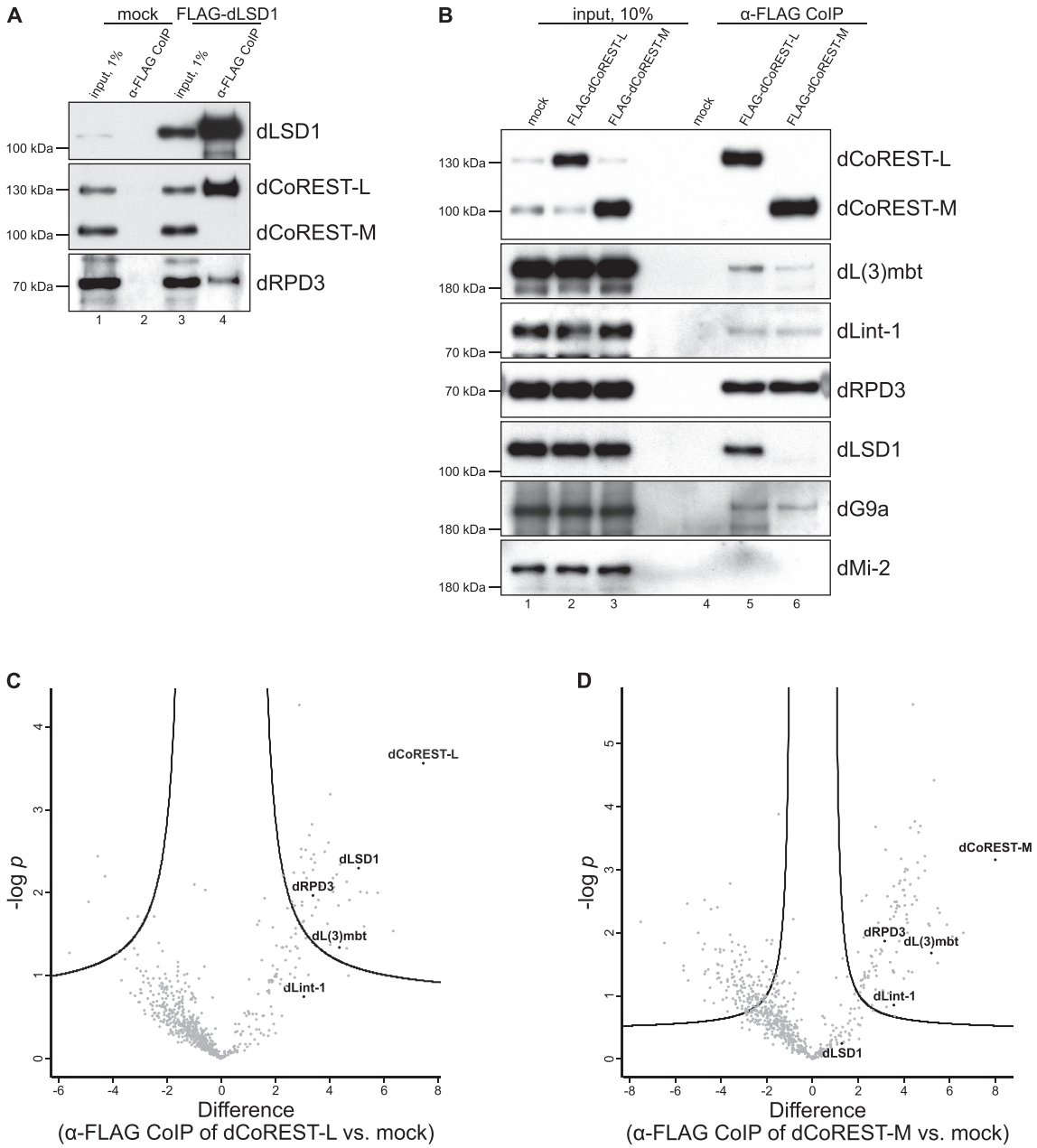

Figure 2. dLSD1 is an isoform-specific dCoREST-L interactor. (**A**) Nuclear extracts from control S2 cells (mock, lanes 1 and 2) and S2 cells stably expressing FLAG-dLSD1 (lanes 3 and 4) were precipitated with anti-FLAG antibody (lanes 2 and 4) and analysed by western blot using the antibodies indicated on the right (lanes 2 and 4). Lanes 1 and 3: 1% input. (**B**) Nuclear extracts from control S2 cells (mock, lanes 1 and 4), S2 cells stably expressing FLAG-dCoREST-L (lanes 2 and 5) or FLAG-dCoREST-M (lanes 3 and 6) were precipitated with anti-FLAG antibody (lanes 4 to 6) and analysed by western blot using antibodies indicated on the right (lanes 4–6). dMi-2 served as a negative control. Lanes 1–3: 10% input. (**C** and **D**) Volcano plot with -log10 *P*-values (*y*-axis) and log2 iBAQ fold-difference (*x*-axis) between the mock control and either the FLAG-CoREST-L affinity purification (C) or the FLAG-CoREST-M affinity purification (D). The complete list of the interacting proteins is presented in Supplementary Tables S2 and 3. ($n = 4$, FDR = 0.2, s0 = 1).

ate two additional cell lines expressing endogenous dG9 with a FLAG-tag at the N-terminus and C-terminus, respectively. Again, anti-FLAG affinity purification followed by SDS/PAGE and silver staining failed to detect interaction partners with apparent molecular masses similar to those of dCoREST or dRPD3 (data not shown). In conclusion, these results identify a dG9a/dCoREST complex but also make clear that the majority of dG9a molecules in nuclear extract are not associated with this complex.

Our proteomic analyses suggest that at least three distinct dCoREST histone deacetylase complexes exist in *Drosophila* which share a common dCoREST/dRPD3 core and are characterized by specific accessory subunits: the LINT complex, a dLSD1/dCoREST complex and a dG9a/dCoREST complex. To provide further support for

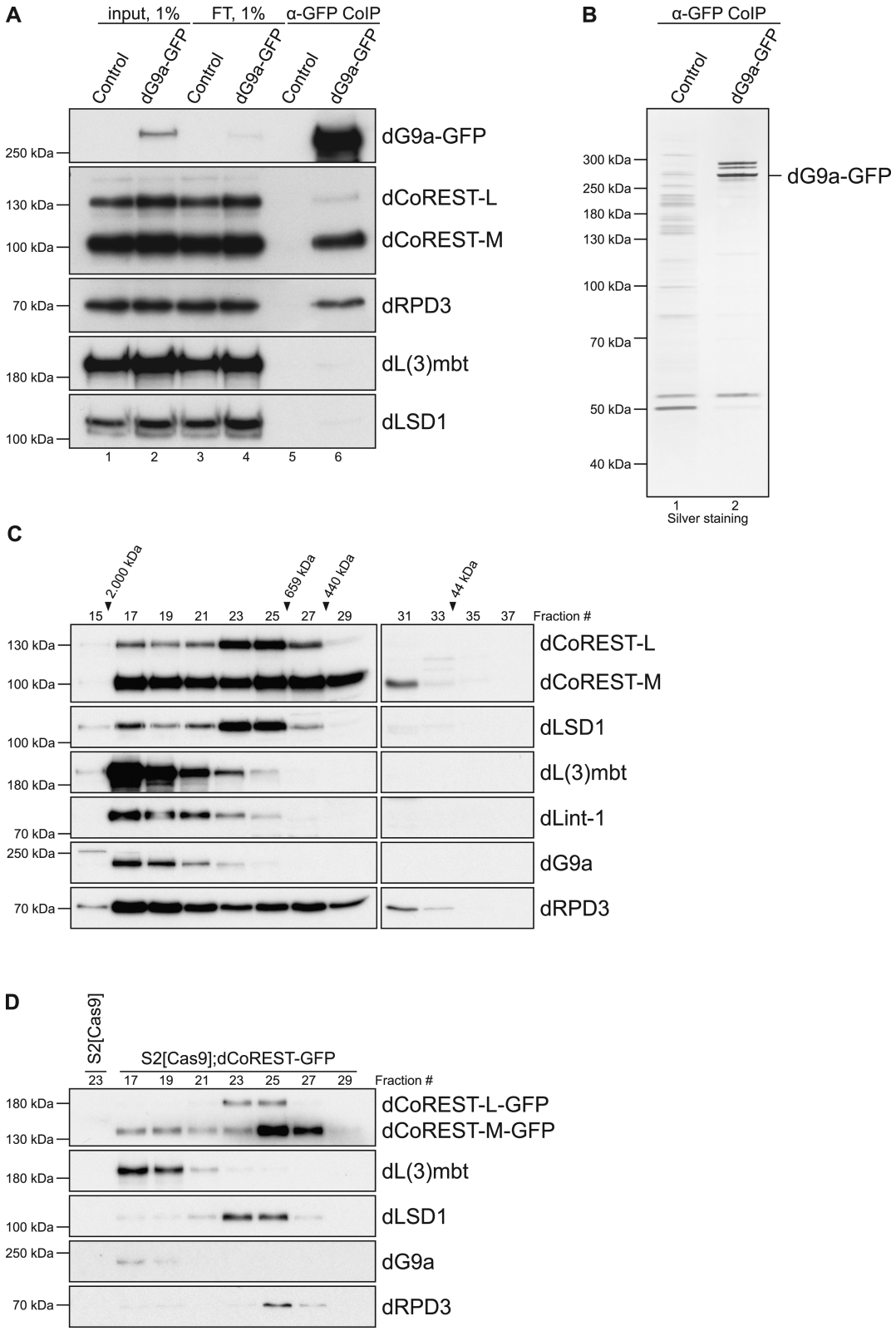

Figure 3. dG9a is a novel dCoREST-interacting protein. (**A**) Nuclear extracts from control S2[Cas9] cells (lanes 1, 3 and 5) and a dG9a-GFP tagged S2[Cas9] cell line (lanes 2, 4 and 6) were precipitated with anti-GFP antibody (lanes 5 and 6) and analysed by western blot using the antibodies indicated on the right. Lanes 1 and 2: 1% input. Lanes 3 and 4: 1% flow through. (**B**) SDS-PAGE and sliver staining of anti-GFP immunopurified nuclear extracts from control S2[Cas9] cells (lane 1) and a dG9a-GFP tagged S2[Cas9] cell line (lane 2). (**C**) A total of 1 mg of nuclear extract from S2 cells was fractionated over a Superose 6 column. Fractions were analysed by western blot using the antibodies indicated on the right. Fraction numbers and molecular mass standards are denoted on top. (**D**) A total of 1 mg of nuclear extract from S2[Cas9];dCoREST-GFP cells was fractionated over a Superose 6 column. Fractions were co-immunoprecipitated using GFP-Trap resin and analysed by western blot using the antibodies indicated on the right. Fraction numbers and molecular mass standards are denoted on top. Fraction #23 from non-tagged parental S2[Cas9] cells was used as a control.

this hypothesis we determined the gel filtration profile for dCoREST, dLSD1, dL(3)mbt, dLint-1, dG9a and dRPD3 using S2 nuclear extract (Figure 3C) and embryo nuclear extract (Supplementary Figure S4). In both cases, dCoREST-L, dCoREST-M and dRPD3 were detected in several fractions representing a broad range of apparent molecular masses (440 to 2000 kDa) in agreement with the notion that these proteins are components of several distinct complexes. dLSD1 and dCoREST-L co-eluted in the same peak fractions (fractions 25 and 19 (S2 nuclear extract); fractions 22 and 23 (embryo nuclear extract) further supporting the hypothesis that dLSD1 and dCoREST-L form a complex. By contrast, dL(3)mbt and dLint-1 peaked in fraction 26 (S2 nuclear extract) and fraction 27 (embryo nuclear extract). dG9a co-eluted with these LINT subunits in S2 nuclear extract (fraction 26) but not in embryo nuclear extract (peak fraction 20). Next, we separated nuclear extracts of S2 cells expressing GFP-tagged dCoREST by gel filtration, immunoprecipitated fractions with GFP antibody and analysed the immunoprecipitates by western blot (Figure 3D). This verified that the dCoREST interaction partners did not only co-elute with dCoREST but were indeed physically associated with dCoREST in their respective gel filtration fractions.

Taken together, three dCoREST-containing complexes can be separated by both immuno-precipitation and gel filtration. This strongly suggests that the dLSD1/dCoREST-L, the LINT and the dG9a/dCoREST complexes can exist as distinct entities. In addition, the similarity of gel filtration profiles derived from S2 nuclear extract and embryo nuclear extract indicates that these complexes are present in different cell types.

Chromatin binding by dCoREST complexes

Our biochemical studies suggest that three separate dCoREST complexes exist in nuclear extract of S2 cells. In order to assess if these assemblies are also associated with chromatin we performed ChIP-seq analyses. We employed CRISPR/Cas-mediated genome editing to generate S2 cell lines expressing GFP-tagged dCoREST, the LINT subunit dL(3)mbt, dLSD1 and dG9a, respectively (Supplementary Figure S3 and Table S5). This allowed us to determine the genome-wide binding profiles for these proteins by ChIP-seq using the same antibody (anti-GFP) in each case. We identified 4855 dCoREST bound sites in the *Drosophila* genome. dCoREST binding sites are greatly enriched in promoters implying a role in the regulation of transcription (Figure 4A). About 73.6% of dCoREST sites are also bound by dL(3)mbt (Figure 4B and D). By contrast, only 17.6 and 18.6% of dCoREST sites are co-occupied by dLSD1 and dG9a, respectively. This suggests that on chromatin the LINT complex is more abundant than either dLSD1/dCoREST or dG9a/dCoREST complexes. About 73.4% of all dL(3)mbt sites are also bound by dCoREST (Figure 4B and D). By contrast, only 10.2 and 7.3% of all dL(3)mbt sites are co-occupied by dLSD1 and dG9a, respectively (Figure 4C). This further supports the notion that the LINT complex is largely distinct from dLSD1/dCoREST and dG9a/dCoREST assemblies. dCoREST is associated with 79.0% of all dLSD1 binding sites (Figure 4B and D). This is in agreement with the notion that the majority of dLSD1 molecules bind chromatin as part of the dLSD1/dCoREST complex and demonstrates that the dLSD1/dCoREST complex associates with chromatin. About 59.0% of all dG9a binding sites are also bound by dCoREST (Figure 4B and D). Whilst this indicates that more than half of dG9a molecules bind chromatin as part of a dG9a/dCoREST assembly it is clear that a significant fraction of dG9a (41.0%) associates with chromatin independently of dCoREST. In conclusion, the comparison of chromatin binding profiles supports the notion that the three dCoREST complexes that we have defined by analysing soluble nuclear extract do indeed form on chromatin.

Gene regulation by CoREST-containing complexes in S2 cells

All three dCoREST complexes identified in our study contain histone modifying enzymes (dRPD3, dLSD1, dG9a) expected to generate closed chromatin structures and to repress gene transcription. Moreover, dCoREST complexes associate predominantly with promoter sequences. Therefore, we next asked what contributions the three dCoREST complexes would make to regulating the transcriptome of S2 cells. We used RNAi-mediated depletion followed by RNA-seq to address this question. S2 cells were treated with double stranded RNAs targeting EGFP (control) and two double stranded RNAs directed against dCoREST. One of these RNAs corresponded to a region shared by both L- and M-isoforms and efficiently depleted both dCoREST-L and dCoREST-M simultaneously (Figure 5A, lane 2). The other RNA hybridized to the insert unique to dCoREST-L and downregulated the dCoREST-L isoform specifically (Figure 5A, lane 3). We noted that depletion of dCoREST-L for four days resulted in slightly reduced western blot signals for most proteins tested suggesting an unspecific effect of dCoREST-L RNAi-treatment on the expression or stability of many proteins (Figure 5A, lane 3). We, therefore, shortened the RNAi treatment to three days (Figure 5A, lanes 8–10). Under these conditions the simultaneous depletion of both dCoREST isoforms as well as the depletion of dCoREST-L alone specifically decreased dLSD1 protein levels without affecting the levels of other proteins. This suggests that dCoREST-L binding to dLSD1 contributes to dLSD1 stability. As we have reported previously, depletion of dL(3)mbt had a similar destabilising effect on dLint-1 ((15); Figure 5A, lane 6).

Simultaneous depletion of both dCoREST-L and dCoREST-M upregulated 668 protein coding genes by a factor of 2.0 or more (log2FC $\geq$ 1) as determined by RNA-seq (Figure 5B). A much smaller number of genes (28) were downregulated. This supports the hypothesis that dCoREST complexes predominantly function to repress transcription. Importantly, 483 (68%) of the genes that change expression upon dCoREST knockdown are bound by dCoREST as determined by ChIP-seq analysis suggesting that these genes are direct targets of dCoREST repressor complexes.

To determine to what extent the three individual dCoREST complexes contribute to gene regulation we analysed

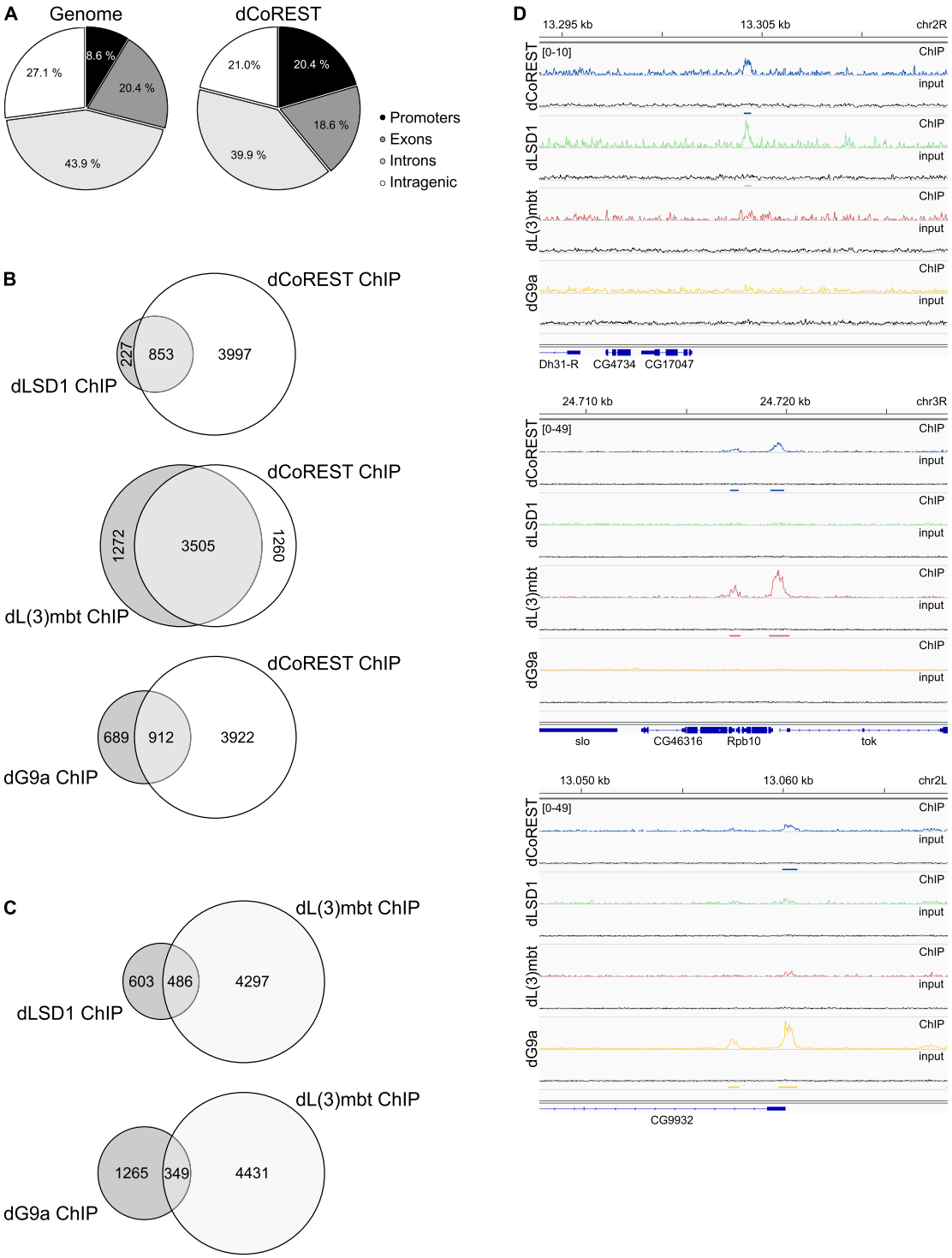

Figure 4. Genome-wide binding profiles of dCoREST, dLSD1, dL(3)mbt and dG9a by ChIP-seq analysis. (**A**) dCoREST binding sites are greatly enriched in promoters. (**B**) Venn diagrams depicting shared and unique ChIP-seq peaks for dCoREST and dLSD1 (top panel), dCoREST and dL(3)mbt (middle panel, and dCoREST and dG9a (bottom panel). (**C**) Venn diagrams depicting shared and unique ChIP-seq peaks for dL(3)mbt and dLSD1 (top panel) and dL(3)mbt and dG9a (bottom panel). Note that one peak of one data set can simultaneously overlap with two or more peaks of the data set it is compared to. As a consequence, the total number of peaks for any given protein is slightly different between Venn diagrams. The actual total numbers of peaks identified are as follows: dCoREST — 4855; dLSD1 — 1126; dL(3)mbt—4785; dG9a—1614). (**D**) Genome browser view of dCoREST and dLSD1 (top panel), dCoREST and dL(3)mbt (middle panel), and dCoREST and dG9a (bottom panel) chromatin associations. Data were visualized with the Integrative Genomics Viewer (Version 2.6.2) and snapshots were taken from representative regions.

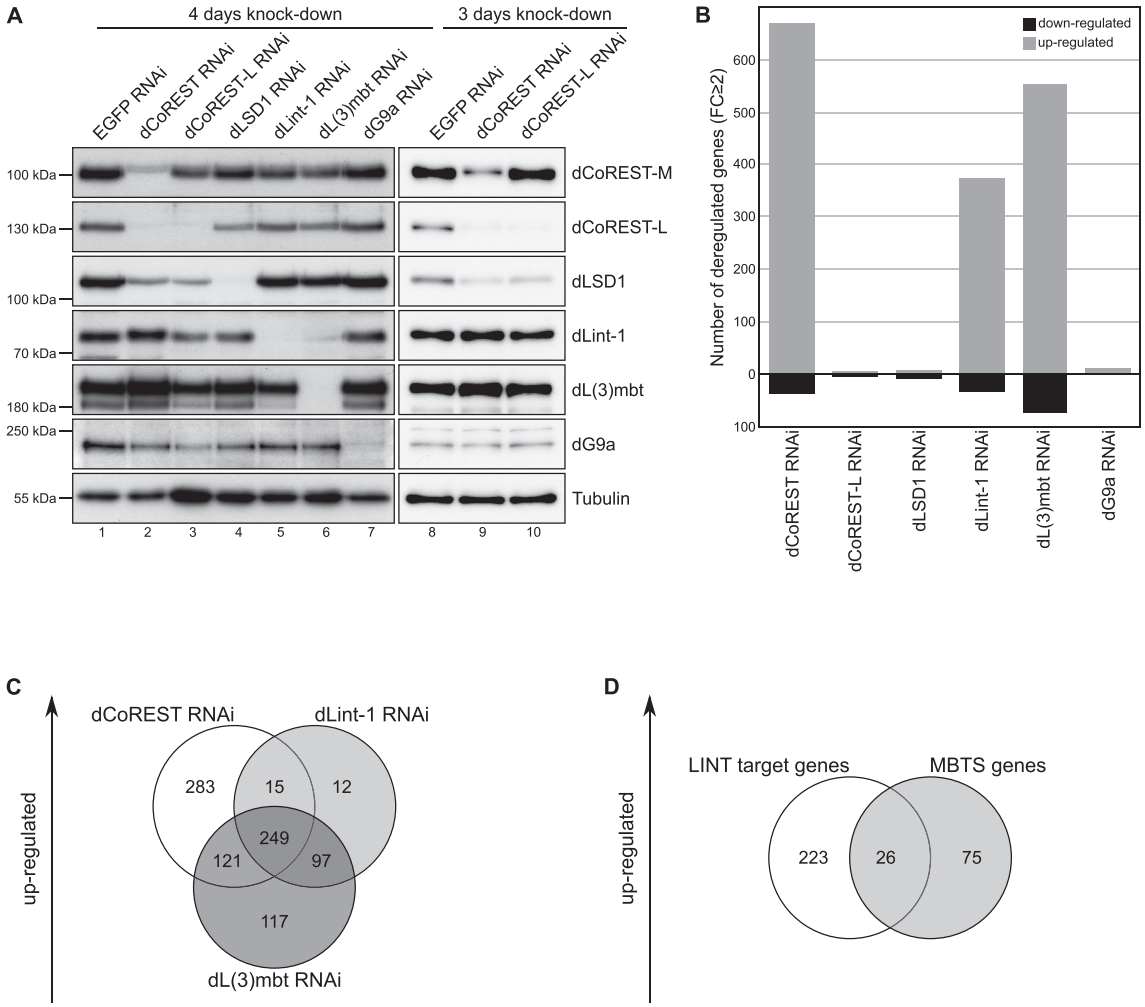

Figure 5. The LINT complex is a major repressor of transcription in S2 cells. S2 cells were treated with dsRNA directed against EGFP, dCoREST, dCoREST-L, dLSD1, dLint-1, dL(3)mbt and dG9a. (**A**) Nuclear extracts of RNAi treated S2 cells were subjected to western blot and analysed using antibodies indicated on the right. (**B**) RNA from these cells was analysed by RNA-seq. The diagram depicts the numbers of down- and upregulated genes (fold change $\geq$2) using transcript levels of EGFP RNAi treated cells as a reference ($n = 3$). (**C**) Venn diagram of genes upregulated upon dCoREST, dL(3)mbt and dLint-1 knockdown (fold change $\geq$2.0, adj. $P \leq 0.05$). (**D**) Venn diagram comparing LINT-repressed genes and malignant brain tumour signature (MBTS) genes.

transcriptomes after depletion of complex-specific subunits (Figure 5A).

Specific depletion of dLSD1 resulted in only few genes being misexpressed (Figure 5B; eight genes upregulated, ten genes downregulated). Likewise, very few genes were misregulated in S2 cells specifically depleted of dCoREST-L (four genes upregulated, four genes downregulated). These results are reminiscent of weak transcriptional effects of LSD1 depletion that have been reported previously: for example, RNAi-mediated depletion of LSD1 in mouse ES cells results in only a weak derepression of LSD1 target genes that does not exceed a factor of 2-fold (29). Therefore, we lowered the threshold of our analysis and considered genes misexpressed by a factor of 1.5 or more (log2FC$\geq$0.58). This, indeed, increased the number of dLSD1-repressed genes to 113 and the number of dCoREST-L-regulated genes to 41 (Supplementary Figure S5). Importantly, 78% of genes upregulated by dCoREST-L depletion were likewise upregulated by dLSD1 depletion suggesting that these genes are indeed repressed by a dLSD1/dCoREST-L complex. Nevertheless, it is clear that the dLSD1/dCoREST-L complex controls a comparatively small proportion of dCoREST-regulated genes in S2 cells even though 853 genomic sites are co-occupied by dCoREST and dLSD1.

Similar to what we observed after depletion of dLSD1, dG9a depletion upregulated only few genes by a factor of 2.0 or more (Figure 5B; 10 genes upregulated, 0 genes downregulated). In this case, including genes that were misregulated by a factor of 1.5-fold or more did not markedly increase the number of affected genes (18 genes upregulated, 16 genes downregulated). We conclude that dG9a does not play a major role in regulating gene transcription in S2 cells.

In stark contrast to the moderate to weak effects of depleting dLSD1/dCoREST complex and dG9a/dCoREST complex-specific subunits, depletion of LINT-specific subunits changed the expression levels of hundreds of genes by a factor of 2.0 or more (Figures 5B; dL(3)mbt: 584 genes upregulated, 56 genes downregulated; dLint-1: 373 genes upregulated, 34 genes downregulated). This suggests that the LINT complex is responsible for the regulation of a large fraction of dCoREST-dependent genes in S2 cells, in agreement with the LINT complex being the predominant chromatin-associated dCoREST complex as demonstrated by ChIP-seq analysis. In support of this hypothesis we find a high degree of overlap between genes that are derepressed by dCoREST, dL(3)mbt or dLint-1 depletion (Figure 5C). A total of 249 genes were upregulated when either dL(3)mbt, dLint-1 or dCoREST was targeted and we consider these to be high confidence LINT targets. Moreover, 385 genes were upregulated in at least two of the three knockdowns. Thus, approximately half of the dCoREST-regulated genes appear to be repressed by the LINT complex. We note that 283 genes are upregulated in dCoREST-depleted cells but neither in dL(3)mbt nor in dLint-1 depleted cells (Figure 5C). At present it is unclear if this is a consequence of a differential requirement for LINT complex subunits at subsets of LINT target genes or if these genes represent targets of as yet unidentified dCoREST complexes.

LINT represses germ line genes in S2 cells

dL(3)mbt and LINT have previously been implicated in the repression of *malignant brain tumour signature* (MBTS) genes. MBTS genes encode mostly germ line-specific proteins that are upregulated in brain tumours of *l(3)mbt* mutant larvae (14–15,30–31). In addition, dL(3)mbt regulates a group of genes targeted by the Salvador-Warts-Hippo (SWH) pathway (31). In agreement with our previous results obtained in Kc cells, LINT-repressed genes in S2 cells included a significant proportion of MBTS genes (26 out of 101) but none of the SWH targets (Figure 5D).

A gene ontology (GO)-term analysis of the 249 high confidence LINT-repressed genes revealed a number of terms that were significantly enriched (Supplementary Figure S6). These included genes linked with the GO-terms "germ line stem cell symmetric division" and "synapsis". Together with our finding that many of the germ line-specific MBTS transcripts are upregulated upon knockdown of LINT subunits, this indicates that LINT functions to repress genes involved in germ cell differentiation in S2 cells.

We had previously determined LINT target genes in Kc cells by microarray analysis (15). Based on the comparative analysis of their transcriptomes, both Kc cells and S2 cells are believed to be derived from embryonal macrophages and LINT might be expected to repress similar sets of genes in both cell lines (32). Indeed, comparison of the LINT regulated genes in Kc and S2 cells revealed a significant degree of overlap (Supplementary Figure S7).

In conclusion, our analyses suggest that LINT shapes the transcriptomes of macrophage-derived cell lines by preventing the inappropriate expression of genes characteristic of other cell types.

Depletion of dCoREST disrupts wing vein differentiation

In order to gain insight into the roles of different dCoREST complexes during fly development we performed RNA interference using the UAS/GAL4 system (33). We investigated two developmental systems, wing and testis, both of which have been shown to be sensitive to mutation or deregulation of several chromatin regulators (10,34–35). For example, RNAi-mediated depletion of dCoREST and dLSD1 throughout the wing imaginal disc has been demonstrated to result in ectopic vein phenotypes (10,36). We used the *engrailed*-GAL4 driver line to direct expression of UAS-shRNA constructs to the posterior half of the developing wing. Indeed, we observed vein phenotypes with high penetrance (100%) when dCoREST was targeted by RNAi (Supplementary Figure S8). Depletion of dLint-1 caused a strong deformation of wing shape that largely precluded an analysis of vein phenotypes. The molecular basis for the dLint-1 phenotype is currently unclear. Whilst depletion of dL(3)mbt, dLSD1 and dG9a did result in vein phenotypes with lower penetrance (<20% of wings analysed), such low penetrance phenotypes were also observed in the driver line (*en*-GAL4) and when RNAi was directed against transcripts unrelated to dCoREST complexes (dChd3, CG9973 and CG2083; Supplementary Figure S8). We therefore conclude that low penetrance vein phenotypes are unlikely to be a specific consequence of depletion of these dCoREST complex subunits. We considered the possibility that the lack of specific phenotypes caused by dL(3)mbt, dLSD1 and dG9a depletion was due to insufficient expression of RNAi constructs. We therefore repeated all crosses and phenotype analyses at an elevated temperature (30°C) known to enhance expression in the UAS-GAL4 system (37). This resulted in an enhancement of the severity of the dCoREST and dLint-1 RNAi phenotypes but still failed to produce specific wing alterations when dL(3)mbt, dLSD1 or dG9a were targeted (Supplementary Figure S9). However, measurement of dL(3)mbt, dLSD1 and dG9a RNA levels in wing discs by qPCR revealed no or only mild RNAi-mediated reductions of expression, precluding us from evaluating the role of these proteins in wing development (data not shown).

Taken together, these results suggest that in our experimental system dCoREST is critical for wing vein differentiation. However, they do not inform on which individual or which combination of the three dCoREST complexes is playing a role.

dLSD1/dCoREST is essential for spermatogenesis

Several of the dCoREST interactors identified in this study have been linked to the regulation of germ cell differentiation: Homozygous dLSD1 mutant females fail to produce oocytes and male flies are infertile (12,38–39). Similarly, mutations in dL(3)mbt, dLint1 and dG9a produce ovary defects and female sterility (14,40). We sought to systematically compare the importance of LINT, dLSD1/dCoREST and dG9a/dCoREST complex subunits for spermatogenesis and male fertility. Towards this end we used the *bag of marbles (bam)* GAL4 driver strain to direct expression of RNAi constructs to germ cells. We first compared

three different RNAi lines expressing shRNA constructs expected to simultaneously downregulate both dCoREST-L and dCoREST-M. Indeed, dCoREST-L and dCoREST-M mRNA expression in testes was reduced to levels ranging from 10 to 35% when these responder lines were crossed to *bam* driver lines (Supplementary Figure S10). Male progeny resulting from these crosses was infertile in agreement with our previous findings (34). This is consistent with the hypothesis that dCoREST-containing complexes are essential for fertility. We then set up a series of crosses to knock down dCoREST, dLSD1, dL(3)mbt, dLint-1 or dG9a in developing male germ cells. To verify efficiency of these knock downs we analysed RNA prepared from testes by qPCR (Supplementary Figure S11 and Table S6). mRNA expression of all RNAi targets was efficiently reduced. We then crossed virgin females with control males or RNAi-depleted males to assess male fertility. Out of 11 lines tested, only dCoREST and dLSD1-depleted males failed to generate offspring (Figure 6A). The fertility of males depleted of dL(3)mbt, dLint-1 or dG9a was indistinguishable from that of controls. This suggests a differential role of dCoREST complexes in male fertility: The dLSD1/dCoREST complex appeared to be essential for fertility whereas both LINT and dG9a/dCoREST complexes seemed dispensable.

Indeed, analysis of testes morphology by phase contrast microscopy revealed that seminal vesicles of control testes contained sperm, whereas seminal vesicles of dCoREST and dLSD1-depleted testes were empty (Figure 6B, panels 1, 2 and 3). Premeiotic spermatocytes did not show any obvious defects (panels 1′, 2′ and 3′). In addition, post meiotic spermatids identified by their flagella extending along a large part of the testis were present in both control and RNAi-depleted testes. This suggests that defects manifest at later stages such as spermatid nuclei elongation, histone-protamine exchange, individualization of sperm or release into the seminal vesicle.

We used immunofluorescence microscopy to identify possible alterations caused by dCoREST and dLSD1 depletion at postmeiotic stages (Figure 6C). During spermiogenesis round spermatid nuclei elongate (canoe stage), individualize and eventually form mature sperm. Histones are removed from DNA and degraded during the canoe stage. Concomitantly protamines and Mst77F are expressed to replace histones in mature sperm (23,28). dCoREST or dLSD1 knockdown did not affect this histone-to-protamine switch as judged by the timely expression and chromatin association of Mst77F. However, spermatid nuclei failed to elongate and no mature, elongated sperm were detected. As hardly any transcription takes place after meiotic divisions, these defects likely are a consequence of aberrant gene regulation during the spermatocyte phase (28). The striking similarity of the phenotypes produced after both dCoREST and dLSD1 knockdowns further strengthens the hypothesis that it is the dLSD1/dCoREST complex that is essential for the cellular processes that govern nuclei elongation.

The dLSD1/dCoREST complex did not appear to be a major regulator of gene transcription in macrophage-like S2 cells (Figure 5). Nevertheless, we hypothesized that it might regulate gene expression during germ cell development. We prepared RNA from bam>>dCoREST RNAi, bam>>dLSD1 RNAi and control testes and analysed their transcriptomes by RNA-seq. In both, dCoREST-depleted and dLSD1-depleted testes, a large number of genes was activated by a factor of 2.0 or more (log2FC≥1; dCoREST-depleted testes: 1721 genes up-regulated, 61 genes downregulated; dLSD1-depleted testes: 1300 genes upregulated, 125 genes downregulated) (Figure 7A). Importantly, 1091 genes were upregulated in both scenarios which corresponds to 63% of all dCoREST-repressed genes and 84% of all dLSD1-repressed genes (Figure 7B). We consider these genes to be high confidence targets of the dLSD1/dCoREST complex. GO-term analysis of these identified 20 GO-terms that were over-represented (Supplementary Figure S12). Eight of these were associated with genes involved in neuron development and function. These findings are consistent with the hypothesis that the dLSD1/dCoREST complex is required to prevent the inappropriate expression of neuron-specific genes in the male germ line.

Collectively, our results demonstrate that dCoREST functions to maintain cell-type-specific gene expression profiles in both macrophage-like S2 cells and in the male germ line. However, to do so different dCoREST complexes are used in a cell-type-specific manner.

DISCUSSION

Multisubunit protein complexes that regulate chromatin often exist as families of complexes with related subunit composition (1). Typically, a set of shared core subunits can associate with diverse complex-specific accessory subunits. Accessory subunits endow complexes with specific functionality by regulating the enzymatic activities of core subunits, adding new enzymatic, nucleosome or RNA binding activities and/or by influencing the targeting to specific genome regions.

Whereas extensive complex families have recently been described for PRC1, PRC2 and SWI/SNF, the number of complexes containing the CoREST repressor that have been identified is comparatively small: In mammalian cells, the bulk of CoREST appears to reside in complexes with LSD1 (6,8,12). Although several studies have found that CoREST can bind additional chromatin regulators it is not clear if these interactions reflect the existence of additional, stable CoREST complexes or are the products of transient binding events. In *Drosophila,* dCoREST and dLSD1 have been shown to interact in ovary extracts and when both proteins are overexpressed in S2 cells (12,13). We have previously identified dCoREST as a subunit of the dL(3)mbt interacting LINT complex (15). In the current study we have used proteomic approaches to systematically determine and characterize the interactome of dCoREST in S2 cells.

Using gel filtration, immunoaffinity purification, mass spectrometry and co-immunoprecipitation approaches we have identified three distinct dCoREST-containing complexes (Figure 8). All three of these complexes contain a heterodimeric core composed of dCoREST itself (either the -L or the -M isoform) and the histone deacetylase dRPD3. This core can associate with additional subunits and histone modifying activities to form either the LINT complex,

A

#	Fly line	Fertile
1	bam-GAL4 driver	+
2	dCoREST RNAi control	+
3	bam>>dCoREST RNAi	-
4	dLSD1 RNAi control	+
5	bam>>dLSD1 RNAi	-
6	dL(3)mbt RNAi control	+
7	bam>>dL(3)mbt RNAi	+
8	dLint-1 RNAi control	+
9	bam>>dLint-1 RNAi	+
10	dG9a RNAi control	+
11	bam>>dG9a RNAi	+

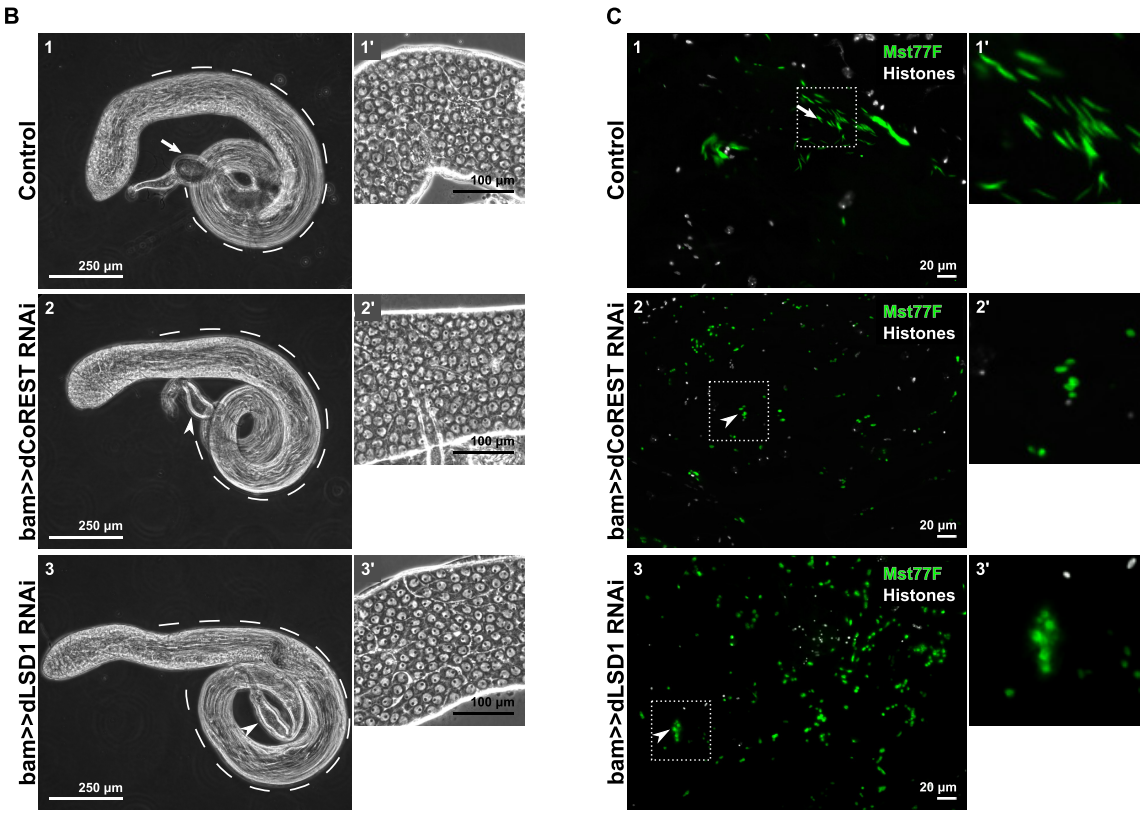

Figure 6. dLSD1/dCoREST complex is essential for spermatogenesis. (**A**) Male fertility tests of control flies and flies in which dCoREST or its interactors were depleted by RNAi ($n = 10$). Only bam>>dCoREST RNAi and bam>>dLSD1 RNAi flies produced no offspring (-). (**B**) Phase contrast images of 1 day old testes from control flies (1 and 1′), bam>>dCoREST RNAi flies (2 and 2′) and bam>>dLSD1 RNAi flies (3 and 3′). Post-meiotic spermatids identified by their flagella extending along a large part of the testis (marked by dashed line) were visible in all testes. Seminal vesicles of control testes (arrow in panel 1) contained sperm, seminal vesicles of RNAi depleted testes were empty (arrowheads in panels 2 and 3). Phase contrast microscopy of spermatocytes of indicated crosses (1′, 2′ and 3′) showed no visible defects. Scale bars: 250 µm (1, 2 and 3) and 100 µm (1′, 2′ and 3′). (**C**) Knockdown of dCoREST and dLSD1 leads to post-meiotic spermatid nuclei elongation defects. Histones (white) and the spermatid-specific protein Mst77F (green) were visualized by immunofluorescence in post-meiotic spermatid nuclei of control testes (1 and 1′) and upon RNAi in bam>>dCoREST RNAi (2 and 2′) and bam>>dLSD1 RNAi (3 and 3′) testes. Scale bars: 20 µm.

a dLSD1/dCoREST complex or a dG9a/dCoREST complex. LINT contains the signature subunits dL(3)mbt and dLint-1, the dLSD1/dCoREST complex is defined by the histone demethylase dLSD1 and the dG9a/dCoREST complex harbours the H3K9 histone methyltransferase dG9a. Thus, all three dCoREST complexes identified in our study have the potential to generate repressive chromatin structures by altering the histone methylation and acetylation status of nucleosomes.

Importantly, the three dCoREST complexes can be separated by immunoprecipitation and gel filtration under mild conditions suggesting that they indeed exist as distinct assemblies in the nucleus. Moreover, ChIP-seq analysis has demonstrated that the majority of dCoREST bound sites

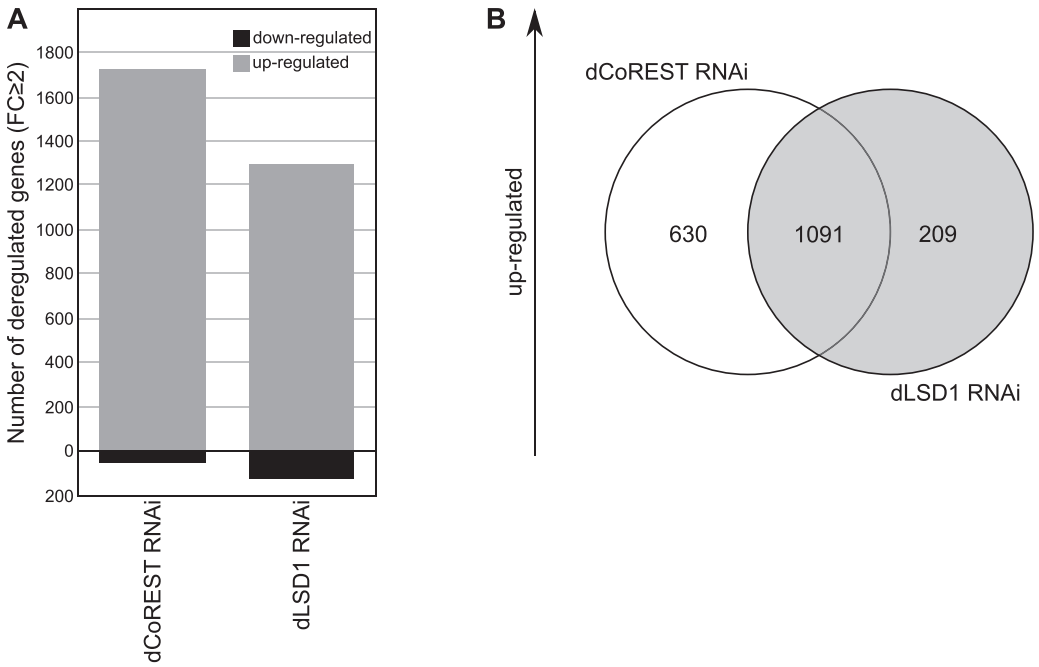

Figure 7. dLSD1/dCoREST complex is a major repressor of transcription during spermatogenesis. (**A**) Bar diagram showing the number of up- and downregulated protein coding genes of testes depleted for dCoREST or dLSD1 as determined by RNA-seq (total 850 testes from at least three biological replicates per condition). (**B**) Venn diagram showing comparison of dCoREST and dLSD1 up-regulated genes (fold change ≥2.0, adj. $P \leq 0.05$).

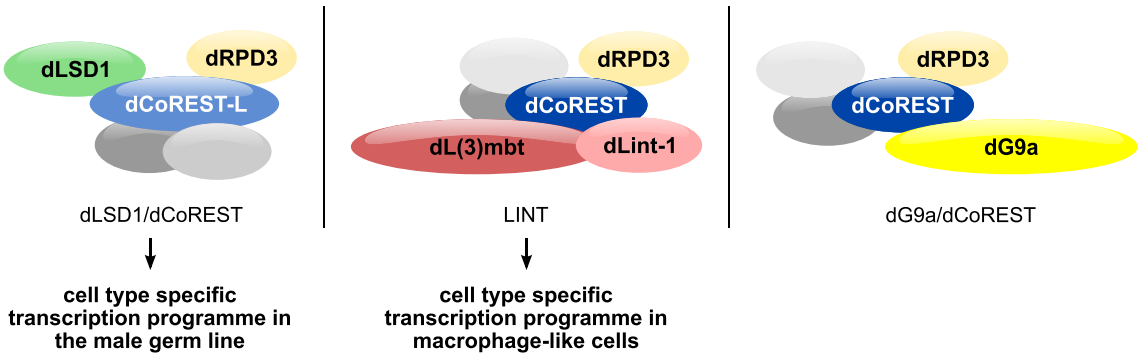

Figure 8. Schematic representation of different dCoREST complexes in Drosophila. Three distinct dCoREST containing complexes share a common dCoREST/dRPD3 core. The dLSD1/dCoREST complex is dCoREST isoform-specific and regulates transcription in the male germ line. The LINT complex is a major repressor of transcription in macrophage-like cells. The targets of the dG9a/dCoREST complex are unknown.

are co-occupied by dL(3)mbt but not by dLSD1 or dG9a further supporting the notion that the complexes associate as independent entities with chromatin. Our proteomic screens for dCoREST interactors have identified additional proteins with established roles in chromatin regulation that we have not yet characterized further. This leaves open the possibility that additional dCoREST-containing complexes might exist.

dCoREST-L and dCoREST-M differ in a 234 aa insertion between the SANT domains that is present in dCoREST-L but not in dCoREST-M (Figure 1A). Our results suggest that both isoforms can be integrated into the LINT and dG9a/dCoREST complexes. By contrast, reciprocal co-immunoprecipitation and reconstitution experiments demonstrate that only dCoREST-L but not dCoREST-M can form a complex with dLSD1. This agrees well with the prior observation that dLSD1 co-immunoprecipitates preferentially with dCoREST-L in ovary extracts. What determines the isoform specificity of this interaction? The structure of a complex formed by fragments of human CoREST and human LSD1 has been solved (41). This structure shows that the interaction surface of CoREST that contacts LSD1 is composed of a part of the region separating the two SANT domains and the second SANT domain itself. Sequence alignment of dCoREST-L with human CoREST reveals conservation across the entire LSD1 contact region (Supplementary Figure S13). The N-terminal part of this region is formed by the dCoREST-L-specific insertion that is missing in dCoREST-M. Thus, a potential explanation for why dCoREST-M cannot stably interact with dLSD1 is that an essential part of the interaction surface is missing in this isoform.

Although human CoREST is also expressed in different alternative splice forms, the strict isoform-specific dLSD1 interaction that we have identified in *Drosophila* does not appear to be conserved: all three major human CoREST isoforms interact with LSD1 (42).

Regulation of alternative splicing is an important mechanism for shaping cell-type-specific proteomes in higher metazoans. It is conceivable that the relative abundance of the three dCoREST complexes in different cell types could be modified by regulating alternative splicing of the dCoREST transcript: increased expression of dCoREST-M at the expense of dCoREST-L would be expected to result in a higher proportion of LINT and dG9a/dCoREST complexes (which can incorporate both isoforms) and a concomitant decrease in dLSD1/dCoREST complex levels. Indeed, the relative expression levels of dCoREST-L and dCoREST-M are significantly different in S2 cells and embryo extracts (compare e.g. Figures 1B, 3C and Supplementary Figure S4), suggesting that regulation of dCoREST expression at the level of alternative splicing might occur.

We have analysed the role of dCoREST complexes in wing development and spermatogenesis and in regulating transcription in the macrophage-like S2 cell line and in the male germ line. In all these settings lowering the expression of dCoREST complexes by RNAi depletion of their shared dCoREST subunits has profound effects on differentiation and changes the transcription of hundreds of genes. In both macrophage-like cells and male germ cells the number of upregulated genes exceeds the number of downregulated genes by a factor of 20-fold or higher. This suggests that dCoREST complexes are important regulators of differentiation in a variety of developmental settings and that they contribute to the maintenance of cell-type-specific transcription programmes predominantly by acting as repressors of transcription.

S2 cells and the male germ line respond with remarkable specificity to the inactivation of individual dCoREST complexes: In macrophage-like S2 cells, depletion of LINT complex signature subunits derepresses hundreds of genes whereas depletion of dLSD1, the dLSD1/dCoREST complex-specific dCoREST-L isoform or dG9a has only minor effects. It remains possible that dLSD1, dCoREST-L and dG9a depletion does lead to small expression changes of weakly expressed genes that our analysis has not been able to detect. In addition, it is possible that dCoREST-L depletion is compensated by dCoREST-M, e.g. by increased binding of dCoREST-M containing complexes to dLSD1/dCoREST-L bound regions. In any case, our study identifies LINT as an important repressor of genes that are inappropriate for macrophages such as the germ line-specific MBTS genes. Our results call into question whether dLSD1 and dG9a play important roles in regulating transcription in macrophage-like cells at all, at least under our experimental conditions, even though they are clearly associated with chromatin and occupy more than a thousand sites. An interesting parallel to our results is the finding that LSD1 knockdown does not result in major transcriptional effects in mouse ES cells (29). This is consistent with the hypothesis that also in mammals the ubiquitous LSD1/CoREST complex regulates transcription in a cell type-restricted manner.

In stark contrast to our results in S2 cells, depletion of dLSD1 (and depletion of dCoREST) results in the derepression of more than 1000 genes in the male germ line, the disruption of spermiogenesis and infertility. Amongst the genes repressed by dLSD1/dCoREST many appear to be specific for non-germ line lineages such as neurons. Depletion of LINT subunits or dG9a has no effect on spermatogenesis. Indeed, LSD1 plays also an important role in mammalian spermatogenesis: The SLC complex containing LSD1, CoREST and SFMB1 is highly expressed in mouse spermatocytes (8). Moreover, LSD1 and SFMBT1 colocalize at meiotic chromosomes. Conditional ablation of LSD1 expression in mouse testis results in misexpression of genes involved in stem cell and progenitor maintenance and differentiation, defective meiosis, complete loss of mature sperm and infertility (43,44). Although these studies did not directly address the role of CoREST these data are consistent with an important role of LSD1/CoREST complexes in spermatogenesis that is remarkably conserved between mouse and fly.

Unlike the LINT and dLSD1/dCoREST complexes for which we have identified important functions as transcriptional regulators in S2 cells and the male germ line, respectively, dG9a depletion did not produce significant effects in any of our experimental systems. These findings agree with earlier studies that have shown that although dG9a is abundantly expressed in the male germ line, dG9a mutants do not display a reduction of H3K9 methylation levels in germ cells (45,46). Moreover, dG9a is a non-essential gene and dG9a null mutants display mostly behavioural phenotypes (47–50). Defects of dG9a deficient flies have been reported under various conditions of stress (50–52). It is conceivable, that the dG9a/dCoREST complex is important in cell types that have not been analysed in our study or exerts its most prominent effects only under particular stress conditions.

A simple explanation for the cell-type- and lineage-specific differences in dCoREST complex function revealed in our study would be a potential differential expression of dCoREST complex signature subunits in S2 cells and testis. Indeed, on the RNA level G9a expression is only moderate in S2 cells and low in testis (Fly Atlas, *data not shown*), thus, providing a potential explanation for the weak effects on transcription when dG9a is depleted in these cells. However, on the protein level, dG9a has been demonstrated to be abundantly expressed in testis (45,46). dLSD1 expression is much higher in S2 cells, where the dLSD1/dCoREST complex represses only few genes, compared to testis, where the dLSD1/dCoREST complex is a major repressor of transcription and essential for spermatogenesis. In addition, dLint-1 expression is higher in testis compared to S2 cells even though depletion of LINT has no effect on spermatogenesis. Taken together, these observations suggest that differences in dCoREST complex repression activity cannot be easily attributed to differences in expression levels.

How is dCoREST complex activity confined to particular cell types and lineages? It is possible that cell-type-specific post-translational modifications of dCoREST complexes activate or inactivate their functions. Alternatively, gene repression by dCoREST complexes might be dependent on cell-type-specific transcription factors that recruit dCoREST complexes to chromatin. These cell-type-specific

transcription factors would specifically interact with one of the dCoREST complexes, potentially by contacting one of their signature subunits, and recruit this complex to sets of genes that need to be silenced in the given cell type. Indeed, we have recently identified such a mechanism involving the germ line-specific transcription factor Kumgang and the chromatin regulator dMi-2 that is responsible for the repression of hundreds of genes in the male germ line (34).

Our study has identified a set of distinct histone deacetylase complexes that are built around a dCoREST/dRPD3 core which have the potential to generate repressive chromatin structures by altering nucleosome acetylation and methylation. These complexes serve to repress lineage inappropriate genes, such as neuronal genes in the male germ line or germ line-specific genes in macrophage-like cells and often play critical roles in differentiation. We have revealed an unexpected division of labour amongst these complexes with individual dCoREST complexes being dedicated to preventing inappropriate gene expression in specific cell lineages and cell types.

In a broader sense, our study adds to the growing appreciation that chromatin regulating complexes are not all purpose machines that exert the same functions in all cell types but, instead, that they are tailored by the inclusion of specific accessory subunits to perform distinct cell type- and lineage-specific roles. Future analyses will aim to define the molecular mechanisms by which this specificity is achieved.

DATA AVAILABILITY

Data generated in this study are available as follows: IP/MS data at ProteomeXchange, identifier PXD014857 (MS identification of dCoREST interactors); raw ChIP-seq data have been deposited in the ArrayExpress database at EMBL-EBI (www.ebi.ac.uk/arrayexpress) under accession number E-MTAB-8341; raw RNA-seq data have been deposited in the ArrayExpress database at EMBL-EBI (www.ebi.ac.uk/arrayexpress) under accession number E-MTAB-7440 (S2 cells) and E-MTAB-7439 (*Drosophila* testes).

SUPPLEMENTARY DATA

Supplementary Data are available at NAR Online.

ACKNOWLEDGEMENTS

We are grateful to Gail Mandel, Gunther Reuter and Masamitsu Yamaguchi for the kind gifts of dCoREST, dLSD1 and dG9a antibodies, respectively, and to Ulla Kopiniak, Corinna Webert, Thomas Plagge and Jonathan Trautwein for experimental assistance. We thank Guntram Suske for critical reading of the manuscript and Peeyush Sahu, Marek Bartkuhn, Robert Liefke and Tobias Zimmermann for assistance with bioinformatic analyses.

FUNDING

Deutsche Forschungsgemeinschaft (DFG) [BR2102/6 to I.M., J.L., A.B.; TRR81/B13 to I.T., T.H., R.R.-P., C.R.; TRR81/A01 to K.K., A.B.]. Funding for open access charge: DFG [TRR81].

Conflict of interest statement. None declared.

REFERENCES

1. Meier,K. and Brehm,A. (2014) Chromatin regulation: how complex does it get? *Epigenetics*, **9**, 1485–1495.
2. Andres,M.E., Burger,C., Peral-Rubio,M.J., Battaglioli,E., Anderson,M.E., Grimes,J., Dallman,J., Ballas,N. and Mandel,G. (1999) CoREST: a functional corepressor required for regulation of neural-specific gene expression. *Proc. Natl. Acad. Sci. U.S.A.*, **96**, 9873–9878.
3. Hakimi,M.A., Bochar,D.A., Chenoweth,J., Lane,W.S., Mandel,G. and Shiekhattar,R. (2002) A core-BRAF35 complex containing histone deacetylase mediates repression of neuronal-specific genes. *Proc. Natl. Acad. Sci. U.S.A.*, **99**, 7420–7425.
4. Humphrey,G.W., Wang,Y., Russanova,V.R., Hirai,T., Qin,J., Nakatani,Y. and Howard,B.H. (2001) Stable histone deacetylase complexes distinguished by the presence of SANT domain proteins CoREST/kiaa0071 and Mta-L1. *J. Biol. Chem.*, **276**, 6817–6824.
5. Lee,M.G., Wynder,C., Cooch,N. and Shiekhattar,R. (2005) An essential role for CoREST in nucleosomal histone 3 lysine 4 demethylation. *Nature*, **437**, 432–435.
6. Shi,Y.J., Matson,C., Lan,F., Iwase,S., Baba,T. and Shi,Y. (2005) Regulation of LSD1 histone demethylase activity by its associated factors. *Mol. Cell*, **19**, 857–864.
7. You,A., Tong,J.K., Grozinger,C.M. and Schreiber,S.L. (2001) CoREST is an integral component of the CoREST- human histone deacetylase complex. *Proc. Natl. Acad. Sci. U.S.A.*, **98**, 1454–1458.
8. Zhang,J., Bonasio,R., Strino,F., Kluger,Y., Holloway,J.K., Modzelewski,A.J., Cohen,P.E. and Reinberg,D. (2013) SFMBT1 functions with LSD1 to regulate expression of canonical histone genes and chromatin-related factors. *Genes Dev.*, **27**, 749–766.
9. Mulligan,P., Yang,F., Di Stefano,L., Ji,J.Y., Ouyang,J., Nishikawa,J.L., Toiber,D., Kulkarni,M., Wang,Q., Najafi-Shoushtari,S.H. *et al.* (2011) A SIRT1-LSD1 corepressor complex regulates Notch target gene expression and development. *Mol. Cell*, **42**, 689–699.
10. Curtis,B.J., Zraly,C.B. and Dingwall,A.K. (2013) Drosophila LSD1-CoREST demethylase complex regulates DPP/TGFbeta signaling during wing development. *Genesis*, **51**, 16–31.
11. Domanitskaya,E. and Schupbach,T. (2012) CoREST acts as a positive regulator of Notch signaling in the follicle cells of Drosophila melanogaster. *J. Cell Sci.*, **125**, 399–410.
12. Lee,M.C. and Spradling,A.C. (2014) The progenitor state is maintained by lysine-specific demethylase 1-mediated epigenetic plasticity during Drosophila follicle cell development. *Genes Dev.*, **28**, 2739–2749.
13. Dallman,J.E., Allopenna,J., Bassett,A., Travers,A. and Mandel,G. (2004) A conserved role but different partners for the transcriptional corepressor CoREST in fly and mammalian nervous system formation. *J. Neurosci.*, **24**, 7186–7193.
14. Coux,R.X., Teixeira,F.K. and Lehmann,R. (2018) L(3)mbt and the LINT complex safeguard cellular identity in the Drosophila ovary. *Development*, **145**, dev160721.
15. Meier,K., Mathieu,E.L., Finkernagel,F., Reuter,L.M., Scharfe,M., Doehlemann,G., Jarek,M. and Brehm,A. (2012) LINT, a novel dL(3)mbt-containing complex, represses malignant brain tumour signature genes. *PLos Genet.*, **8**, e1002676.
16. Kunert,N. and Brehm,A. (2008) Mass production of Drosophila embryos and chromatographic purification of native protein complexes. *Methods Mol. Biol.*, **420**, 359–371.
17. van den Berg,D.L., Snoek,T., Mullin,N.P., Yates,A., Bezstarosti,K., Demmers,J., Chambers,I. and Poot,R.A. (2010) An Oct4-centered protein interaction network in embryonic stem cells. *Cell Stem Cell*, **6**, 369–381.
18. Schmidt,A., Forne,I. and Imhof,A. (2014) Bioinformatic analysis of proteomics data. *BMC Syst. Biol.*, **8**, S3.
19. Rathke,C., Barckmann,B., Burkhard,S., Jayaramaiah-Raja,S., Roote,J. and Renkawitz-Pohl,R. (2010) Distinct functions of Mst77F and protamines in nuclear shaping and chromatin condensation during Drosophila spermiogenesis. *Eur. J. Cell Biol.*, **89**, 326–338.
20. Murawska,M., Kunert,N., van Vugt,J., Langst,G., Kremmer,E., Logie,C. and Brehm,A. (2008) dCHD3, a novel ATP-dependent

chromatin remodeler associated with sites of active transcription. *Mol. Cell Biol.*, **28**, 2745–2757.
21. Dobin,A., Davis,C.A., Schlesinger,F., Drenkow,J., Zaleski,C., Jha,S., Batut,P., Chaisson,M. and Gingeras,T.R. (2013) STAR: ultrafast universal RNA-seq aligner. *Bioinformatics*, **29**, 15–21.
22. Love,M.I., Huber,W. and Anders,S. (2014) Moderated estimation of fold change and dispersion for RNA-seq data with DESeq2. *Genome Biol.*, **15**, 550.
23. Rathke,C., Baarends,W.M., Jayaramaiah-Raja,S., Bartkuhn,M., Renkawitz,R. and Renkawitz-Pohl,R. (2007) Transition from a nucleosome-based to a protamine-based chromatin configuration during spermiogenesis in Drosophila. *J. Cell Sci.*, **120**, 1689–1700.
24. Hundertmark,T., Theofel,I., Eren-Ghiani,Z., Miller,D. and Rathke,C. (2017) Analysis of chromatin dynamics during drosophila spermatogenesis. *Methods Mol. Biol.*, **1471**, 289–303.
25. Livak,K.J. and Schmittgen,T.D. (2001) Analysis of relative gene expression data using real-time quantitative PCR and the 2(-Delta Delta C(T)) Method. *Methods*, **25**, 402–408.
26. Bottcher,R., Hollmann,M., Merk,K., Nitschko,V., Obermaier,C., Philippou-Massier,J., Wieland,I., Gaul,U. and Forstemann,K. (2014) Efficient chromosomal gene modification with CRISPR/cas9 and PCR-based homologous recombination donors in cultured Drosophila cells. *Nucleic Acids Res.*, **42**, e89.
27. Scharf,A.N., Meier,K., Seitz,V., Kremmer,E., Brehm,A. and Imhof,A. (2009) Monomethylation of lysine 20 on histone H4 facilitates chromatin maturation. *Mol. Cell Biol.*, **29**, 57–67.
28. Rathke,C., Baarends,W.M., Awe,S. and Renkawitz-Pohl,R. (2014) Chromatin dynamics during spermiogenesis. *Biochim. Biophys. Acta*, **1839**, 155–168.
29. Nair,V.D., Ge,Y., Balasubramaniyan,N., Kim,J., Okawa,Y., Chikina,M., Troyanskaya,O. and Sealfon,S.C. (2012) Involvement of histone demethylase LSD1 in short-time-scale gene expression changes during cell cycle progression in embryonic stem cells. *Mol. Cell Biol.*, **32**, 4861–4876.
30. Janic,A., Mendizabal,L., Llamazares,S., Rossell,D. and Gonzalez,C. (2010) Ectopic expression of germline genes drives malignant brain tumor growth in Drosophila. *Science*, **330**, 1824–1827.
31. Richter,C., Oktaba,K., Steinmann,J., Muller,J. and Knoblich,J.A. (2011) The tumour suppressor L(3)mbt inhibits neuroepithelial proliferation and acts on insulator elements. *Nat. Cell Biol.*, **13**, 1029–1039.
32. Cherbas,L., Willingham,A., Zhang,D., Yang,L., Zou,Y., Eads,B.D., Carlson,J.W., Landolin,J.M., Kapranov,P., Dumais,J. *et al.* (2011) The transcriptional diversity of 25 Drosophila cell lines. *Genome Res.*, **21**, 301–314.
33. Brand,A.H. and Perrimon,N. (1993) Targeted gene expression as a means of altering cell fates and generating dominant phenotypes. *Development*, **118**, 401–415.
34. Kim,J., Lu,C., Srinivasan,S., Awe,S., Brehm,A. and Fuller,M.T. (2017) Blocking promiscuous activation at cryptic promoters directs cell type-specific gene expression. *Science*, **356**, 717–721.
35. Kovac,K., Sauer,A., Macinkovic,I., Awe,S., Finkernagel,F., Hoffmeister,H., Fuchs,A., Muller,R., Rathke,C., Langst,G. *et al.* (2018) Tumour-associated missense mutations in the dMi-2 ATPase alters nucleosome remodelling properties in a mutation-specific manner. *Nat. Commun.*, **9**, 2112.
36. Curtis,B.J., Zraly,C.B., Marenda,D.R. and Dingwall,A.K. (2011) Histone lysine demethylases function as co-repressors of SWI/SNF remodeling activities during Drosophila wing development. *Dev. Biol.*, **350**, 534–547.
37. Duffy,J.B. (2002) GAL4 system in drosophila: a fly geneticist's Swiss army knife. *Genesis*, **34**, 1–15.
38. Rudolph,T., Yonezawa,M., Lein,S., Heidrich,K., Kubicek,S., Schafer,C., Phalke,S., Walther,M., Schmidt,A., Jenuwein,T. *et al.* (2007) Heterochromatin formation in Drosophila is initiated through active removal of H3K4 methylation by the LSD1 homolog SU(VAR)3-3. *Mol. Cell*, **26**, 103–115.
39. Szabad,J., Reuter,G. and Schroder,M.B. (1988) The effects of two mutations connected with chromatin functions on female germ-line cells of Drosophila. *Mol. Gen. Genet.*, **211**, 56–62.
40. Lee,K.S., Yoon,J., Park,J.S. and Kang,Y.K. (2010) Drosophila G9a is implicated in germ cell development. *Insect Mol. Biol.*, **19**, 131–139.
41. Yang,M., Gocke,C.B., Luo,X., Borek,D., Tomchick,D.R., Machius,M., Otwinowski,Z. and Yu,H. (2006) Structural basis for CoREST-dependent demethylation of nucleosomes by the human LSD1 histone demethylase. *Mol. Cell*, **23**, 377–387.
42. Barrios,A.P., Gomez,A.V., Saez,J.E., Ciossani,G., Toffolo,E., Battaglioli,E., Mattevi,A. and Andres,M.E. (2014) Differential properties of transcriptional complexes formed by the CoREST family. *Mol. Cell Biol.*, **34**, 2760–2770.
43. Lambrot,R., Lafleur,C. and Kimmins,S. (2015) The histone demethylase KDM1A is essential for the maintenance and differentiation of spermatogonial stem cells and progenitors. *FASEB J.*, **29**, 4402–4416.
44. Myrick,D.A., Christopher,M.A., Scott,A.M., Simon,A.K., Donlin-Asp,P.G., Kelly,W.G. and Katz,D.J. (2017) KDM1A/LSD1 regulates the differentiation and maintenance of spermatogonia in mice. *PLoS One*, **12**, e0177473.
45. Stabell,M., Eskeland,R., Bjorkmo,M., Larsson,J., Aalen,R.B., Imhof,A. and Lambertsson,A. (2006) The Drosophila G9a gene encodes a multi-catalytic histone methyltransferase required for normal development. *Nucleic Acids Res.*, **34**, 4609–4621.
46. Ushijima,Y., Inoue,Y.H., Konishi,T., Kitazawa,D., Yoshida,H., Shimaji,K., Kimura,H. and Yamaguchi,M. (2012) Roles of histone H3K9 methyltransferases during Drosophila spermatogenesis. *Chromosome Res.*, **20**, 319–331.
47. Anreiter,I., Kramer,J.M. and Sokolowski,M.B. (2017) Epigenetic mechanisms modulate differences in Drosophila foraging behavior. *Proc. Natl. Acad. Sci. U.S.A.*, **114**, 12518–12523.
48. Kramer,J.M., Kochinke,K., Oortveld,M.A., Marks,H., Kramer,D., de Jong,E.K., Asztalos,Z., Westwood,J.T., Stunnenberg,H.G., Sokolowski,M.B. *et al.* (2011) Epigenetic regulation of learning and memory by Drosophila EHMT/G9a. *PLoS Biol.*, **9**, e1000569.
49. Seum,C., Bontron,S., Reo,E., Delattre,M. and Spierer,P. (2007) Drosophila G9a is a nonessential gene. *Genetics*, **177**, 1955–1957.
50. Shimaji,K., Konishi,T., Tanaka,S., Yoshida,H., Kato,Y., Ohkawa,Y., Sato,T., Suyama,M., Kimura,H. and Yamaguchi,M. (2015) Genomewide identification of target genes of histone methyltransferase dG9a during Drosophila embryogenesis. *Genes Cells*, **20**, 902–914.
51. An,P.N.T., Shimaji,K., Tanaka,R., Yoshida,H., Kimura,H., Fukusaki,E. and Yamaguchi,M. (2017) Epigenetic regulation of starvation-induced autophagy in Drosophila by histone methyltransferase G9a. *Sci. Rep.*, **7**, 7343.
52. Merkling,S.H., Bronkhorst,A.W., Kramer,J.M., Overheul,G.J., Schenck,A. and Van Rij,R.P. (2015) The epigenetic regulator G9a mediates tolerance to RNA virus infection in Drosophila. *PLoS Pathog.*, **11**, e1004692.